

Review

# Reactivity of Basaltic Minerals for CO<sub>2</sub> Sequestration via In Situ Mineralization: A Review

Muhammad Hammad Rasool \*  and Maqsood Ahmad \* 

Petroleum Geosciences Department, Universiti Teknologi Petronas, Bandar Seri Iskander 32610, Perak, Malaysia  
\* Correspondence: muhammad\_19000949@utp.edu.my (M.H.R.); maqsood.ahmad@utp.edu.my (M.A.)

**Abstract:** The underground storage of CO<sub>2</sub> (carbon dioxide) in basalt presents an exceptionally promising solution for the effective and permanent sequestration of CO<sub>2</sub>. This is primarily attributed to its geochemistry and the remarkable presence of reactive basaltic minerals, which play a pivotal role in facilitating the process. However, a significant knowledge gap persists in the current literature regarding comprehensive investigations on the reactivity of basaltic minerals in the context of CO<sub>2</sub> sequestration, particularly with respect to different basalt types. To address this gap, a comprehensive investigation was conducted that considered seven distinct types of basalts identified through the use of a TAS (total alkali–silica) diagram. Through a thorough review of the existing literature, seven key factors affecting the reactivity of basaltic minerals were selected, and their impact on mineral reactivity for each basalt type was examined in detail. Based on this analysis, an *M.H. reactivity scale* was introduced, which establishes a relationship between the reactivity of dominant and reactive minerals in basalt and their potential for carbonation, ranging from low (1) to high (5). The study will help in choosing the most suitable type of basalt for the most promising CO<sub>2</sub> sequestration based on the percentage of reactive minerals. Additionally, this study identified gaps in the literature pertaining to enhancing the reactivity of basalt for maximizing its CO<sub>2</sub> sequestration potential. As a result, this study serves as an important benchmark for policymakers and researchers seeking to further explore and improve CO<sub>2</sub> sequestration in basaltic formations.

**Keywords:** basalt; mineral reactivity; *M.H. reactivity scale*; mineralization; CO<sub>2</sub> storage



**Citation:** Rasool, M.H.; Ahmad, M. Reactivity of Basaltic Minerals for CO<sub>2</sub> Sequestration via In Situ Mineralization: A Review. *Minerals* **2023**, *13*, 1154. <https://doi.org/10.3390/min13091154>

Academic Editors: Rafael Santos, Shaoping Chu and Rajesh J. Pawar

Received: 24 June 2023

Revised: 10 August 2023

Accepted: 11 August 2023

Published: 31 August 2023



**Copyright:** © 2023 by the authors. Licensee MDPI, Basel, Switzerland. This article is an open access article distributed under the terms and conditions of the Creative Commons Attribution (CC BY) license (<https://creativecommons.org/licenses/by/4.0/>).

## 1. Introduction

Atmospheric CO<sub>2</sub> (carbon dioxide) concentrations have reached unprecedented levels in human history, surpassing 423.6 ppm in 2023 from a preindustrial level of 280 ppm. This increase has occurred at a rate of approximately 2.3 ppm per year over the past decade, which is about 100 times faster than natural variations [1,2]. The primary driver behind the rising CO<sub>2</sub> concentrations is the extensive use of fossil fuels, leading to an enhanced greenhouse effect that elevates global average temperatures and impacts various systems, including climate, ecology, and society. To mitigate these effects, the 2015 Paris Agreement sets a target of limiting anthropogenic warming to 1.5–2 °C [3,4]. Consequently, it is crucial to find solutions that effectively and consistently reduce the net flow of CO<sub>2</sub> into the atmosphere while ensuring the fulfillment of energy requirements [5,6]. The International Energy Agency suggests that the goals of the Paris Agreement can be accomplished by maximizing the practical limits of existing climate-mitigation technologies [7]. These climate-mitigation techniques include submitting Nationally Determined Contributions (NDCs) that outline specific emission reduction targets and strategies, transitioning to renewable energy sources, enhancing energy efficiency, implementing carbon pricing mechanisms, promoting carbon capture and storage (CCS), conserving and restoring forests, and prioritizing adaptation and resilience measures. The Paris Agreement recognizes the need for comprehensive and ambitious actions to address climate change and promote a sustainable future [8].

Numerous geological systems worldwide possess the capacity to securely retain CO<sub>2</sub> captured from industrial activities for centuries [9,10]. Basalt formations possess superior CO<sub>2</sub> storage efficiency compared to other geological formations, thanks to their remarkable reactivity, widespread availability, and geological durability [11–13]. The reactive minerals found in basalt facilitate rapid and effective mineral carbonation, enabling efficient storage of CO<sub>2</sub> [7,14]. Additionally, the abundance of basalt deposits worldwide offers ample opportunities for large-scale implementation of CO<sub>2</sub> storage initiatives [15–17]. Basalt's structural stability and long-term resilience make it an appealing choice for long-term CO<sub>2</sub> storage, contributing significantly to global efforts to reduce greenhouse gas emissions and combat climate change [18–20]. Basalt's capacity to permanently sequester CO<sub>2</sub> makes it an appealing choice for carbon capture and storage (CCS) strategies [21,22]. Once the CO<sub>2</sub> is stored in basalt formations, it remains trapped within the mineralized rock, preventing its re-emission into the atmosphere [20,23–25]. There are certain limitations and uncertainties associated with the CO<sub>2</sub> storage in basalt; however, its potential of rapid mineralization and carbonation instills confidence in the efficacy of basalt reservoirs as a viable solution for mitigating greenhouse gas emissions [26,27]. Moreover, basalt formations offer geological stability and containment integrity. Basalt is known for its variable permeability, reducing the risk of CO<sub>2</sub> leakage [27,28]. The dense structure of basalt hinders the migration of CO<sub>2</sub> through fractures, ensuring the confinement of the stored CO<sub>2</sub> within the reservoir [29,30]. This geological stability enhances the safety and security of the storage operation [31,32].

The reactivity of minerals plays a crucial role in the process of CO<sub>2</sub> carbonation, which has significant implications for mitigating climate change and developing sustainable carbon capture and storage technologies [33,34]. Carbonation involves the chemical reaction between CO<sub>2</sub> and minerals to form stable carbonate compounds. The reactivity of minerals determines the rate and extent of this carbonation process [35–37]. Minerals that possess high reactivity towards CO<sub>2</sub> are desirable for efficient carbonation [38]. These reactive minerals, such as olivine, serpentine, or certain types of basalt, contain elements like magnesium, calcium, or iron, which readily react with CO<sub>2</sub> to form solid carbonate minerals [39]. The carbonation reaction involves the dissolution of CO<sub>2</sub> in water to form carbonic acid (H<sub>2</sub>CO<sub>3</sub>), which then reacts with the mineral surface to release metal cations (e.g., Mg<sup>2+</sup>, Ca<sup>2+</sup>, Fe<sup>2+</sup>) and form stable carbonate minerals (e.g., magnesium carbonate, calcium carbonate, iron carbonate) [40].

The role of mineral reactivity in CO<sub>2</sub> carbonation is twofold. Firstly, highly reactive minerals accelerate the rate of carbonation, facilitating the capture and conversion of CO<sub>2</sub> into stable carbonate compounds [41,42]. This fast carbonation kinetics are desirable for efficient carbon capture and storage systems, as they enable a rapid transformation of CO<sub>2</sub> into solid forms, effectively immobilizing it and reducing its potential for atmospheric release [43,44]. Secondly, the reactivity of minerals affects the overall carbonation capacity [45–47]. Minerals with higher reactivity can sequester more CO<sub>2</sub> by providing a larger surface area for reaction and a greater availability of reactive sites. The overall carbonation capacity of minerals is influenced by their reactivity, which determines how effectively they can chemically react with CO<sub>2</sub> to form stable carbonate compounds. Minerals with higher reactivity possess a greater ability to absorb and sequester CO<sub>2</sub> through carbonation [48]. In context of intrinsic reactivity, surface area, and in situ mineralization, it is important to understand that minerals with higher reactivity have the potential to sequester more CO<sub>2</sub>. This is due to their larger surface area, which provides increased availability of reactive sites. However, it is crucial to recognize that intrinsic reactivity is influenced by factors such as mineral composition and crystal structure. Moreover, the surface area of minerals plays a significant role in facilitating the contact between CO<sub>2</sub> and minerals, influencing the carbonation reaction rate and overall efficiency. This understanding is particularly relevant in the context of in situ mineralization, as the assessment of carbonation potential within geological formations relies on considerations of intrinsic reactivity and surface area [49]. Understanding and optimizing the reactivity of minerals in CO<sub>2</sub> carbonation are vital for advancing carbon capture and storage technologies. Researchers are

actively investigating methods to enhance mineral reactivity, such as mechanical activation, thermal treatment, or chemical pre-treatment [50,51]. These techniques aim to increase the surface area, modify the mineral structure, or introduce catalytic additives to improve the efficiency of carbonation processes.

Despite the importance of the reactivity of basalt minerals in the carbonation and mineralization process, thorough study on the reactivity of the minerals present in different kinds of basalt is lacking. The development of efficient carbon capture and storage methods is hampered by our inadequate understanding of particular mineralogical compositions and their related reactivity potentials. Therefore, there is a critical information vacuum regarding the detailed research of basalt minerals and their reactivity, which hinders the optimization of carbon sequestration technology and restricts our capacity to successfully battle climate change.

#### *Various Routes of CO<sub>2</sub> Sequestration in Basalt*

CO<sub>2</sub> sequestration in basalt involves various routes and methods that leverage the reactivity of basaltic minerals to capture and store carbon dioxide. Here are some different routes for CO<sub>2</sub> sequestration in basalt.

**In Situ Mineral Carbonation:** In this method, CO<sub>2</sub> is injected deep into underground basalt formations that are porous and permeable. Once injected, the CO<sub>2</sub>-rich fluids come into contact with the minerals in the basalt, leading to a series of chemical reactions. The CO<sub>2</sub> dissolves in water to form carbonic acid, which reacts with minerals like olivine, pyroxenes, and feldspars in the basalt. These reactions result in the formation of stable carbonate minerals, such as calcite, magnesite, and serpentine. These carbonates are securely stored in the geological formations, effectively sequestering the captured CO<sub>2</sub> [52].

**Enhanced Weathering:** Enhanced weathering aims to accelerate the natural weathering process of basaltic rocks by exposing them to the atmosphere and CO<sub>2</sub>-rich fluids. This can be achieved by spreading crushed basalt on land surfaces or using ocean-based platforms to increase exposure. Rainwater or CO<sub>2</sub>-enriched solutions interact with the basaltic minerals, leading to mineral dissolution and the subsequent formation of carbonate minerals. The carbonation reactions lock up the CO<sub>2</sub> in stable mineral forms [53].

**Direct Injection into Basalt Aquifers:** Injection of CO<sub>2</sub> into deep underground basalt aquifers involves injecting CO<sub>2</sub> into formations that already contain water. The injected CO<sub>2</sub> dissolves in the water, creating carbonic acid that reacts with the minerals in the basalt. This reaction leads to the dissolution of minerals and the precipitation of carbonate minerals, which are stored in the aquifer over time [54,55].

**Subsurface Injection with Hydrothermal Activation:** This method combines CO<sub>2</sub> injection with the injection of hot water into basalt formations. The heat from the injected water enhances the reactivity of the minerals in the basalt, leading to faster dissolution and carbonation reactions. Hydrothermal conditions accelerate the mineral carbonation reactions and can improve overall carbon capture efficiency [56].

**Ocean-Based Sequestration:** Some proposals suggest grinding basaltic rocks into fine particles and dispersing them in the ocean. The fine particles react with dissolved CO<sub>2</sub> in seawater to form carbonate minerals. This process can contribute to ocean carbon sequestration and potentially mitigate ocean acidification [57].

**Hydrothermal Mineralization:** Hydrothermal processes involve subjecting basaltic rocks to high-temperature and high-pressure conditions. These conditions promote rapid mineral dissolution and the subsequent formation of carbonate minerals. Hydrothermal mineralization may be applicable in regions where suitable geothermal resources are available [58].

**Coupling with Geothermal Energy:** Basalt formations with access to geothermal resources can use the heat from these resources to accelerate mineral carbonation reactions. Geothermal fluids are utilized to heat water, enhancing the reactivity of basaltic minerals and promoting the formation of carbonate minerals [59].

**Hydraulic Fracturing and CO<sub>2</sub> Injection:** In this approach, hydraulic fracturing techniques are employed to create fractures in basalt formations. These fractures provide pathways for the injection of CO<sub>2</sub>-rich fluids. The injected CO<sub>2</sub> interacts with the minerals in the fractured basalt, leading to mineral carbonation reactions [60].

This study focusses on the critical review and analysis of the reactivity of basaltic minerals and their in situ CO<sub>2</sub> carbonation potentials. Seven different types of basalt based on their mineralogical composition have been identified based on a TAC diagram. The reactivity of basaltic minerals has been reviewed in the context of CO<sub>2</sub> sequestration. Seven independent factors, i.e., temperature and pressure, fluid pH, rock composition, fluid composition, dissolution rate, grain size and surface area, and geological settings have been identified from literature that affect the carbonation process, and the reactivity of all basalt types has been analyzed based on these parameters. These factors are further categorized into two sections, i.e., reactivity and favorability factors. Lastly, an *M.H. reactivity scale* has been introduced which features the reactivity of dominant minerals in these basalt types directly relating to their carbonation potential.

## 2. Importance of Understanding the Geochemistry of Basalt for CO<sub>2</sub> Storage

A thorough understanding of basalt geochemistry is essential for the effectiveness of CO<sub>2</sub> storage programs. Geochemical processes occurring in basaltic rocks play an important role in determining the long-term fate and stability of CO<sub>2</sub> storage [61,62]. Understanding the interactions between CO<sub>2</sub> and basaltic materials on a geochemical scale will allow researchers and engineers to optimize storage systems and ensure the long-term viability of carbon sequestration. Mineral carbonization processes are an important aspect of basaltic geochemistry [63]. Through this process, CO<sub>2</sub> chemically reacts with minerals present in the basalt, forming carbonate minerals [64–68]. The rate and extent of mineral charring depends on various factors such as temperature, pressure, water availability and basalt mineral composition [69–71]. By examining these parameters, scientists can identify the optimal conditions for increasing carbonation rates, thereby maximizing CO<sub>2</sub> storage efficiency.

Furthermore, understanding the geochemistry of basalts will help assess potential risks and challenges associated with CO<sub>2</sub> storage [72–74]. Factors such as the presence of reactive minerals in basalts can induce mineral alterations that can affect the overall stability and durability of CO<sub>2</sub> storage. Gaining insight into these geochemical processes will allow the scientist to develop strategies to mitigate risks such as deposits and clogging, thereby ensuring the long-term integrity of CO<sub>2</sub> storage [75]. In addition, a thorough understanding of basalt geochemistry helps in selecting suitable sites for CO<sub>2</sub> storage. Basalt layers exhibit differences in mineral composition, porosity, and permeability [75,76]. These properties influence the suitability of a particular basalt reservoir for CO<sub>2</sub> storage. Through detailed geochemical analysis, researchers can identify basalt formations with optimal properties such as high reactivity, low permeability, and favorable water–rock interactions. With this knowledge, choosing the right storage location will ensure effective and safe CO<sub>2</sub> storage. In summary, understanding basalt geochemistry is essential for successful CO<sub>2</sub> storage programs. This enables optimization of storage systems, assessment of potential risks, and selection of suitable storage sites, ensuring long-term stability and availability of CO<sub>2</sub> storage. By combining geological and geochemical knowledge, scientists and engineers can advance their development and implementation of CO<sub>2</sub> storage in basalt formations, helping to mitigate greenhouse gas emissions and combat climate change.

### 2.1. Geochemical Composition of Basalt

The geochemical makeup of basalt is intricate and varied, encompassing a wide array of elements, minerals, and isotopes [77–79]. Basalt predominantly consists of dark-colored minerals like pyroxene, olivine, and plagioclase feldspar, which contribute to its distinct appearance. However, the specific geochemical composition of basalt can exhibit significant variations influenced by factors such as its origin, the type of volcanic activity involved, and the geological evolution of the region [80–83].

Among the major elements present in basalt, silicon (Si), oxygen (O), aluminum (Al), iron (Fe), magnesium (Mg), calcium (Ca), sodium (Na), and potassium (K) hold substantial significance [84–86]. These elements combine to form a diverse range of minerals, with silicate minerals being the most prevalent [87]. Silica ( $\text{SiO}_2$ ) plays a vital role in the composition of basalt, affecting its overall characteristics [88]. Basalt can be classified into different categories, such as tholeiitic basalt and alkaline basalt, based on variations in silica content [88]. Additionally, trace elements assume importance in the geochemical composition of basalt. Although present in smaller quantities, these elements exert significant influence on various processes, including  $\text{CO}_2$  storage. Examples of trace elements found in basalt include chromium (Cr), nickel (Ni), copper (Cu), zinc (Zn), and cobalt (Co) [89–91]. The presence and distribution of these trace elements offer insights into the origins and evolution of basaltic magma and the potential interactions with  $\text{CO}_2$  during storage. Isotopic compositions of specific elements, such as carbon (C), oxygen (O), and sulfur (S), can also be utilized in the study of basalt's geochemical characteristics [92–94]. Stable isotopes like carbon-13 ( $^{13}\text{C}$ ) and oxygen-18 ( $^{18}\text{O}$ ) provide valuable information about the sources and processes involved in basalt formation [95]. Isotopic ratios and fractionation patterns aid in distinguishing between different basaltic sources and offer insights into the interaction of basalt with  $\text{CO}_2$  and other fluids during storage [96,97]. A comprehensive understanding of the geochemical composition of basalt is crucial for various applications, including  $\text{CO}_2$  storage. It enables scientists to evaluate the reactivity of basaltic minerals, assess the suitability of specific basalt formations for  $\text{CO}_2$  storage, and predict the long-term behavior of stored  $\text{CO}_2$ . Additionally, geochemical analysis assists in identifying potential risks associated with basalt storage, drilling through basalts with appropriate drilling methods and drilling fluids [98–102] and problems such as mineral alterations or the release of hazardous elements.

## 2.2. Categorization of Basalts Based on Their Geochemistry

The geochemistry of basalts can be categorized using a variety of classification techniques. The total alkali–silica (TAS) diagram, which plots the weight percent of silica ( $\text{SiO}_2$ ) against the total weight percents of sodium oxide ( $\text{Na}_2\text{O}$ ) and potassium oxide ( $\text{K}_2\text{O}$ ), is one of the most often used classification schemes. This illustration aids in the distinction between tholeiitic basalts, alkaline basalts, and other forms of basalt. It is important to keep Johannsen's (1937) [103] perspective in mind before utilizing the (total alkali–silica) TAS or any other classification scheme for igneous rocks, i.e., '*numerous and diverse classifications have been proposed, reflecting the varied purposes they serve and the inherent complexities of the rocks themselves. The challenges in classification arise not from the systems themselves, but from the inherent imperfections of nature. Nevertheless, rock classification is necessary to facilitate comparisons with previously described rocks of similar composition and appearance. When a genetic basis is lacking, an artificial system becomes a useful tool, functioning as a card index for rock descriptions. While such artificial systems may be viewed as less ideal, they are often the best available option among several alternatives*'.

Furthermore, as extensively discussed by Le Maitre and others (2002) [104], it is essential to recognize that the classification, including the TAS diagram, cannot be universally applied to all volcanic rocks. Certain rocks are unsuited for classification using this diagram, and for those, additional criteria based on chemical, mineralogical, or textural attributes must be employed, as exemplified by lamprophyres [105]. It is crucial to limit the application of the TAS classification to rocks where the mineral mode cannot be determined. In cases where mineralogy can be established, alternative schemes based on mineralogical compositions, such as the QAPF (Quartz, Alkali feldspar, Plagioclase, Feldspathoid) diagram or other diagrams specific to igneous rocks, should be utilized [106,107]. Prior to classifying rocks using the TAS diagram, it is necessary to recalculate chemical analyses to a total of 100%, excluding water and  $\text{CO}_2$  [108–110]. As a part of this review paper, seven basalt types have been identified based on their alkali and silica content and have been plotted on TAS diagram as shown in Figure 1 and are summarized in Table 1. It is

important to note here that TAS diagram does not relate to mineralization capacity, but rather simply relates to basalt classification.

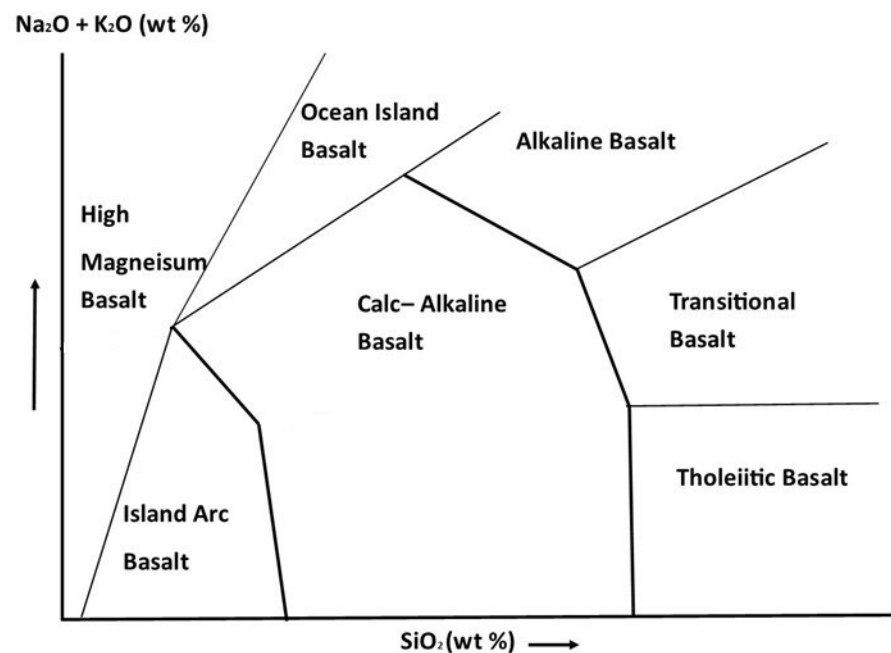


**Figure 1.** TAS diagram for identification of seven basalt types based on their silica and alkali content.

Based on the Figure 1, the following common basalt categories are listed and discussed further:

**Alkaline basalts** are distinguished by their high sodium (Na<sub>2</sub>O) and/or potassium (K<sub>2</sub>O) concentrations. They typically contain less silica than other forms of basalt and are present in the alkali field of the TAS diagram. Alkaline basalts are found in volcanic environments including continental rift zones and oceanic islands [111–113].

**Tholeiitic basalts** are characterized by relatively low concentrations of sodium and potassium. They are present in the tholeiitic field of the TAS diagram and have moderate to high silica content. Tholeiitic basalts are commonly associated with mid-ocean ridges and continental flood basalt provinces [114–116].

**Transitional basalts** exhibit geochemical characteristics between alkaline basalts and tholeiitic basalts. They are present in the transition zone between the alkali and tholeiitic fields on the TAS diagram. Transitional basalts are often associated with areas of tectonic transition or magmatic evolution [117,118].

**High-magnesium basalts**, also known as boninites or picrites, are characterized by elevated magnesium (MgO) content and low silica content. They typically have high concentrations of magnesium oxide and are present outside the alkali and tholeiitic fields on the TAS diagram. HMB basalts are associated with tectonic environments such as subduction zones [93,119–121].

**Calc-alkaline basalts** are characterized by a combination of calc-alkaline and tholeiitic geochemical signatures. They typically have higher aluminum (Al<sub>2</sub>O<sub>3</sub>) and lower magnesium (MgO) contents compared to tholeiitic basalts. Calc-alkaline basalts are often associated with volcanic arcs and subduction zones [122–124].

**Ocean island basalts** are associated with hotspots or mantle plumes and are characterized by distinct geochemical signatures. They often have higher concentrations of incompatible elements, such as niobium (Nb) and tantalum (Ta), and low concentrations of high field strength elements (HFSEs) compared to other basalts [125–127].

**Island arc basalts** are typically found in volcanic arcs associated with subduction zones. They show a geochemical signature characterized by enrichments in trace elements

such as lead (Pb) and thallium (Tl), as well as high ratios of large ion lithophile elements (LILEs) to high field strength elements (HFSEs) [128–130].

**Table 1.** Categorization of basalt based on geochemistry.

Basalt Type	Mineralogy		Major Elements	Trace Elements	Petrography
Alkaline basalts	Plagioclase feldspar	30%–45%	Na <sub>2</sub> O, K <sub>2</sub> O, SiO <sub>2</sub>	Nb, Rb, Th, U, LREE, Ba, Sr, Zr, Hf	Fine to coarse-grained texture with small mineral crystals
	Pyroxene	20%–40%			
	Olivine	5%–30%			
	Amphibole	<5%			
Tholeiitic Basalts	Plagioclase feldspar	40%–70%	FeO, MgO, SiO <sub>2</sub>	Ni, Cr, Sc, V, Ti, P, Zn, Co, Mn	Porphyritic texture with phenocrysts in a fine-grained matrix
	Pyroxene	20%–40%			
	Olivine	5%–25%			
	Magnetite	5%–15%			
Transitional Basalts	Plagioclase feldspar	30%–50%	Na <sub>2</sub> O, K <sub>2</sub> O, FeO, MgO, SiO <sub>2</sub>	REE, Ti, P, Zr, Hf, Ba, Sr, Nb, Rb, Th, U	Variable textures (porphyritic, intersertal, aphanitic)
	Pyroxene	20%–40%			
	Olivine	5%–25%			
	Alkali Feldspar and clinopyroxene	<5%			
	Magnetite	5%–15%			
High-Magnesium Basalts	Olivine	30%–60%	MgO, SiO <sub>2</sub>	Ni, Cr, Co, Mn, Sc, V	Large olivine phenocrysts with a fine-grained groundmass
	Pyroxene	10%–40%			
	Plagioclase Feldspar	<10%			
	Spinifex texture	<5%			
Calc-alkaline Basalts	Plagioclase feldspar	10%–40%	Al <sub>2</sub> O <sub>3</sub> , SiO <sub>2</sub> , FeO, MgO	Pb, Tl, Sr, Ba, Rb, Zr, Hf, LREE, HFSEs	Porphyritic texture with visible phenocrysts
	Pyroxene	20%–30%			
	Olivine	5%–25%			
	Amphibole	<5%			
	Magnetite	5%–15%			
Ocean Island Basalts	Plagioclase feldspar	10%–40%	FeO, MgO, SiO <sub>2</sub>	Nb, Ta, K, Pb, Th, U, LREE, HFSEs	Aphanitic to porphyritic texture
	Pyroxene	10%–40%			
	Olivine	40%–50%			
	Amphibole	<5%			
	Magnetite	5%–15%			
Island Arc Basalts	Plagioclase feldspar	30%–60%	Al <sub>2</sub> O <sub>3</sub> , SiO <sub>2</sub> , FeO, MgO	Pb, Tl, Ba, Sr, Rb, LREE, HFSEs, LILEs	Variable textures (aphanitic, porphyritic, vesicular)
	Pyroxene	10%–40%			
	Olivine	5%–25%			
	Amphibole	<5%			
	Magnetite	<5%			

### 2.3. Major Minerals in Basalt

The main minerals found in the aforementioned varieties of basalt exhibit varying degrees of reactivity. There are three major minerals in basalt, i.e., plagioclase, olivine, and pyroxene, and are commonly found in all types of basalt in different percentages. Various basaltic minerals are discussed below.

Therefore, minerals with higher surface areas tend to exhibit greater reactivity in carbonation processes. Plagioclase exhibits high dissolution rates but has comparatively larger grain sizes. On the other hand, olivine and pyroxene have lower dissolution rates, but their surface area is high. When considering carbonation, dissolution rates become more important. Therefore, among all basaltic minerals, plagioclase is ranked as the most reactive, followed by feldspathoid, olivine, and then pyroxene. It is important to note that this ranking is a general simplification of the reactivity of these minerals. Various other factors, such as pH, fluid composition, temperature (T), and pressure (P), influence the reactivity of these minerals, which are discussed further in the formulation of *M.H. reactivity scale*.

**Plagioclase Feldspar:** Found in basalt in both calcium- and sodium-rich variants, plagioclase feldspar can have a variety of chemical compositions. Plagioclase belongs to the feldspar group and is classified as a series of tectosilicate minerals. Unlike a single mineral with a distinct chemical composition, plagioclase represents a continuous solid solution series, referred to as the plagioclase feldspar series, within which various compositions exist. The composition of a plagioclase feldspar is commonly indicated by its relative proportion of anorthite (%An) or albite (%Ab). Some major minerals in plagioclase series are albite, oligoclase, andesine, labradorite, bytownite, and anorthite. Within the plagioclase feldspar series, there exist several named feldspars that lie between the compositions of albite and anorthite. Plagioclase feldspar's composition affects its reactivity. While sodic plagioclase can undergo more extensive alteration, such as sericitization or saussuritization, under low-grade hydrothermal conditions, calcic plagioclase is often less reactive [35,37].

**Olivine:** Olivine is a ferromagnesian mineral that is highly reactive and susceptible to alteration. It can undergo hydration reactions, leading to the formation of secondary minerals like serpentine, talc, or chlorite. The alteration of olivine to these secondary minerals is commonly observed in weathered or hydrothermally altered basaltic rocks [35,44,131]. Pure Olivine contains the following: olivine:  $(\text{Mg, Fe})_2\text{SiO}_4$  (86.4%), enstatite:  $\text{MgSiO}_3$  (6.3%), magnesiochromite:  $\text{MgCr}_2\text{O}_4$  (1.3%), quartz:  $\text{SiO}_2$  (0.5%), serpentine:  $\text{Mg}_3\text{Si}_2\text{O}_5(\text{OH})_4$  (1.4%), clinocllore:  $(\text{Mg, Fe}^{2+})_5\text{Al}(\text{Si}_3\text{Al})\text{O}_{10}(\text{OH})_8$  (2.3%), talc:  $\text{Mg}_3\text{Si}_4\text{O}_{10}(\text{OH})_2$  (0.8%), and actinolite:  $\text{Ca}_2(\text{Mg, Fe}^{2+})_5\text{Si}_8\text{O}_{22}(\text{OH})_2$  (1.0%) [132].

**Pyroxene:** Basalt frequently contains pyroclastic minerals like clinopyroxene and orthopyroxene. Members of pyroxene family have a complex chemical composition that encompasses elements such as iron, magnesium, aluminum, and others. These elements are bonded to polymerized silica tetrahedra, forming chains, sheets, or three-dimensional structures. The interconnected tetrahedra share corner oxygen atoms, resulting in polymers. Pyroxenes are commonly found in mafic igneous rocks like peridotite, basalt, and gabbro, as well as metamorphic rocks such as eclogite and blue schist.

The structure of pyroxenes consists of long chains of polymerized silica tetrahedra, where each tetrahedron shares two corner oxygens. Metal cations facilitate the bonding between silica chains, leading to the formation of crystal structures. Augite, a well-known member of the pyroxene family, displays various solid solution series and possesses a complex chemical formula  $(\text{Ca,Na})(\text{Mg,Fe,Al,Ti})(\text{Si,Al})_2\text{O}_6$ , which gives rise to multiple mineral names within the pyroxene family. Pyroxene's reactivity might change depending on the particular mineral makeup. Although clinopyroxene is often less reactive than olivine, it can nonetheless go through changes that lead to the development of secondary minerals such as amphibole or serpentine [16,133].

**Spinel:** Some forms of basalt, such as komatiites, include spinel, a trace mineral. Spinel can be found as a metamorphic mineral in transformed limestones and mudstones with low silica content. It is also present as a primary mineral in rare mafic igneous rocks. In these igneous rocks, the magma lacks sufficient alkalis in comparison with aluminum, resulting in the formation of corundum or the combination of aluminum oxide with magnesia to form spinel. This association explains why spinel and ruby are often discovered together. The origins of spinel in mafic magmatic rocks are subject to considerable debate, but it is

believed to result from the interaction of mafic magma with more evolved magma or rock types like gabbro or troctolite.

Spinel, represented by the chemical formula  $(Mg,Fe)(Al,Cr)_2O_4$ , is commonly found in peridotite within the uppermost layers of the Earth's mantle, ranging from approximately 20 km to around 120 km in depth, with the possibility of occurrence at even greater depths depending on its chromium content. At shallower depths, above the Moho discontinuity, calcic plagioclase is the stable aluminous mineral in peridotite, while deeper within the mantle, below the spinel stability region, garnet becomes the prevailing phase. In comparison with olivine or pyroxene, it is more stable and less reactive. Spinel has a stronger resistance to chemical breakdown and can endure weathering and modification processes [134–136].

**Feldspathoids, such as leucite and nepheline:** The feldspathoids are a cluster of tectosilicate minerals that bear resemblance to feldspars, yet possess distinct structures and considerably lower silica content. These minerals are uncommon and typically found in rare and peculiar forms of igneous rocks, often absent in rocks that contain primary quartz. Feldspathoid minerals can substitute for or be present in addition to feldspar in alkaline basalts and some transitional basalts. In comparison to feldspars, feldspathoids are often less stable and more reactive.

#### 2.4. Reactivity of Trace Elements in Basalt

The reactivity of trace elements in basalt can vary depending on several factors, including their chemical properties, environmental conditions, and the presence of other minerals or fluids. The general overview of the reactivity of some common trace elements found in basalt is given below [137–139]:

**Iron (Fe):** Iron is a relatively reactive element, especially in the presence of oxygen and water. It can undergo oxidation reactions, leading to the formation of iron oxides or hydroxides.

**Manganese (Mn):** Manganese can exhibit varying reactivity depending on its oxidation state. Manganese can undergo oxidation reactions, forming manganese oxides or hydroxides.

**Titanium (Ti):** Titanium is generally considered relatively stable and less reactive. However, under specific conditions, such as high-temperature hydrothermal environments, titanium can participate in redox reactions and form titanium oxides.

**Chromium (Cr):** Chromium is typically stable and relatively unreactive under normal geological conditions. However, in oxidizing environments, it can undergo oxidation reactions and form chromate or dichromate compounds.

**Nickel (Ni):** Nickel is generally considered relatively stable in basaltic environments. However, under certain conditions, such as high-temperature hydrothermal systems, nickel can undergo sulfide mineralization or form nickel-bearing minerals.

**Copper (Cu):** Copper can exhibit variable reactivity depending on environmental conditions. In oxidizing environments, it can undergo oxidation reactions and form copper oxides or hydroxides.

**Zinc (Zn):** Zinc is generally stable and less reactive in basaltic environments. It can form secondary zinc minerals under specific hydrothermal conditions.

**Lead (Pb):** Lead is typically considered relatively stable and unreactive in basaltic environments. However, it can undergo alteration or incorporation into secondary minerals under specific circumstances.

#### 2.5. Factors Influencing Mineralization Reactions in Basalt (Parameters for M.H. reactivity scale)

The mineralization reactions occurring in basalt can be influenced by multiple factors. The following factors will be used to formulate a M.H reactivity scale that will help in choosing the most suitable type of basalt based on the percentage composition of reactive minerals. The following are some important variables that can affect the mineralization process [140–143]:

**Temperature and Pressure:** The mineralization process is greatly influenced by temperature. Different minerals have a range of stable temperatures within which they can form or change into other minerals. Lower temperatures may prevent or delay mineralization processes, whereas higher temperatures may promote faster reaction rates and the creation of some minerals.

The stability and mineral formation of minerals can be impacted by pressure circumstances. Phase transitions, which cause minerals to crystallize or change into distinct mineral phases, can be brought on by variations in pressure. Specific mineral assemblages can form as a result of high pressure conditions, as those present in subduction zones.

**Dissolution Rate:** The dissolution rate of minerals refers to how quickly a mineral dissolves in a fluid, such as water or CO<sub>2</sub>-rich solutions. Minerals with higher dissolution rates will react more readily with CO<sub>2</sub> to form carbonates. While this factor does influence the overall reactivity, it is not the sole determinant.

**Fluid Composition:** The composition of fluids interacting with basalt can greatly influence mineralization reactions. Fluids can introduce new elements or compounds into the system, leading to the precipitation of specific minerals or the dissolution and reprecipitation of existing minerals. The presence of different ions, such as metals or sulfur, in the fluid can drive mineralization processes.

**Fluid pH and Redox Conditions:** pH and redox conditions play a crucial role in determining the types of minerals that can form. Varying pH levels can promote the precipitation or dissolution of specific minerals. Redox conditions, such as the presence of oxidizing or reducing agents, can control the stability and formation of certain mineral phases.

**Grain size and surface area:** The carbonation reaction of minerals is intricately related to both grain size and surface area. Smaller grain sizes result in larger surface areas per unit mass, which translates into faster reaction rates, enhanced reactivity, and reduced diffusion distances. As a consequence, the increased surface area allows for more contact between minerals and CO<sub>2</sub>, leading to improved kinetics and greater efficiency in the carbonation process.

**Rock Composition:** The composition of the basalt itself, including the types and relative proportions of minerals present, can impact mineralization reactions. Different minerals have varying reactivities and susceptibilities to alteration, which can influence the formation of secondary minerals during mineralization processes.

**Geological Setting:** The geological setting in which the basalt is found can provide specific conditions and processes that influence mineralization. For example, hydrothermal systems associated with volcanic activity or metamorphic environments can create unique conditions for mineralization to occur.

The above factors are divided into two categories, i.e., reactivity factors and favorability factor as shown in Figure 2. Grain size and dissolution rate will describe the overall reactivity of the minerals and the carbonation potential of the basalt thus named as 'reactivity factors'. Other factors such as geological setting, rock composition, fluid pH, fluid composition, temperature, and pressure are 'favorability factors', which indirectly affect the reactivity of basaltic minerals. There are three major minerals, i.e., plagioclase, olivine, and pyroxene, and are commonly found in all types of basalt in different percentages. This discussion focuses on the reactivity of essential minerals, as summarized in Table 2. The reactivity of basaltic minerals is determined based on their dissolution rate and grain size that will further help in assigning reactivity rating to different basalt types. Various research group have utilized various methodologies to report dissolution rates [144], but one of the most reliable ways is to report the dissolution rates in terms of weathering of metal ions [145–147].

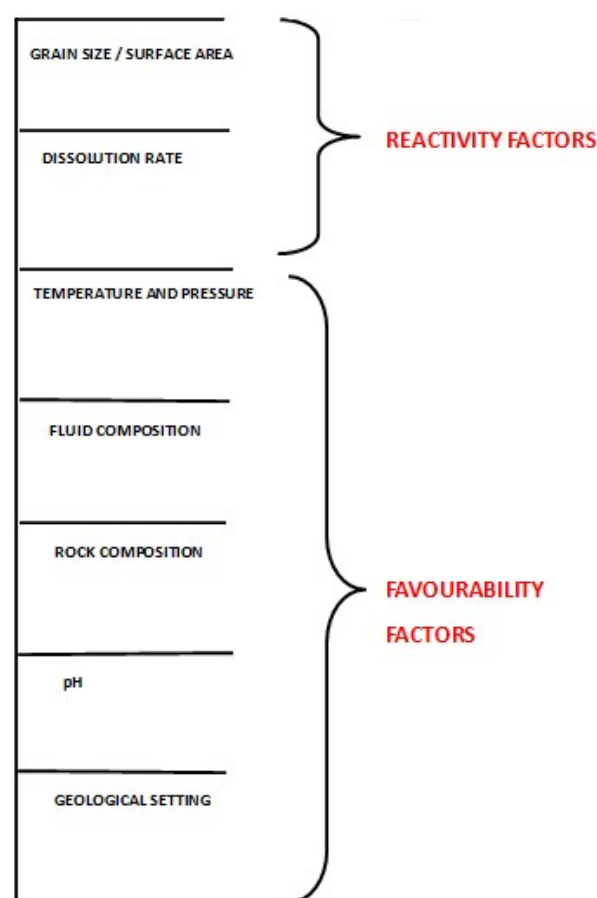


**Figure 2.** *M.H. reactivity scale* parameters for choosing basalt type for CO<sub>2</sub> storage.

Plagioclase exhibits high dissolution rates but has comparatively larger grain sizes. On the other hand, olivine and pyroxene have lower dissolution rates, but their surface area is high. It is important to note that this ranking shown in Table 2 is a general simplification of the reactivity of these minerals. Various proofs from literature on grain size and reaction kinetics of minerals in context of CO<sub>2</sub> sequestration are reported in Table 3. Various other factors, such as pH, fluid composition, temperature (T), and pressure (P), influence the reactivity of these minerals indirectly, which are discussed further in the formulation of *M.H. reactivity scale*.

**Table 2.** Comparative reactivity of basaltic minerals as a function of two intrinsic properties, i.e., grain size and dissolution rate for carbonation [145–148].

Mineral	Dissolution Rate (NaCl Buffered) at 25 °C (mol/m <sup>2</sup> /s) (pH 4–5)				Overall Dissolution Rating	Grain Size Area mm <sup>2</sup> (No. of Samples)	Surface Area	Overall Reactivity
	Si <sup>2+</sup>	Mg <sup>2+</sup>	Ca <sup>2+</sup>	Al <sup>3+</sup>				
<b>Plagioclase</b>	$5.92 \times 10^{-11}$	-	$1.79 \times 10^{-10}$	$9.90 \times 10^{-11}$	High	0.81(65) High	Low	High to Moderate
<b>Olivine</b>	$2.38 \times 10^{-13}$	$1.62 \times 10^{-12}$	-	-	Low	0.50(28) Low	High	Moderate to Low
<b>Pyroxene</b>	$1.62 \times 10^{-13}$	$6.5 \times 10^{-11}$	$8.2 \times 10^{-10}$	-	Moderate	0.52(65) Moderate	Moderate	Moderate

**Table 3.** Studies on grain size and reaction kinetics of major basaltic minerals in context of CO<sub>2</sub> sequestration.

Author/Year	Methodology	Minerals Studied	Findings
Mohalid et al. (2022) [149]	CO <sub>2</sub> sequestration through mineral carbonation using Fe-rich mine waste.	Fe-rich mineral	A particle size of <38 µm resulted in 83.8 g CO <sub>2</sub> /kg being sequestered, with smaller particle sizes highly favoring the carbonation process
Alexandar et al. (2017) [150]	Studied reaction variables in the dissolution of serpentine for mineral carbonation	Serpentine	The study suggests that reducing the particle size to <168 µm enhances structural defects within the silicate crystal lattice, leading to increased exposure of labile magnesium, primarily attributed to the expanded surface area
Zirandi et al. (2017a) [151]	Mineral carbonation of ultramafic mining wastes	Ultramafic formation	A trend of decreasing grain size and increasing reactivity of heterogeneous rock samples was reported
Zirandi et al. (2017b) [152]	Ambient mineral carbonation of different lithologies	Various lithologies	The finer the median particle size, the better the kinetics were observed in all four lithologies
Harrison et al., 2015 [153]	Kinetic of brucite-doped quartz column under elevated CO <sub>2</sub> conditions	Brucite	Higher conversion of brucite and apparent kinetics are obtained using very fine and fine particles
Kelemen et al., 2011 [154]	Calculation of mineral dissolution rates using grain size data	Wollastonite	Wollastonite is a fast-reacting silicate mineral suitable for carbonation, but economic deposits are limited, making it impractical for large-scale CO <sub>2</sub> storage due to high costs
Matter and Kelemen, 2009 [155]	Calculation of mineral dissolution rates using grain size data	Olivine	Olivine, a major mineral constituent of the upper mantle, reacts rapidly with CO <sub>2</sub> -bearing fluids, making it a crucial mineral for CO <sub>2</sub> mineralization processes
O'Connor et al., 2005 [156]	Experimental carbonation of wollastonite	Wollastonite (CaSiO <sub>3</sub> )	The study suggests that olivine-rich ultramafic rocks, such as mantle peridotite, are highly favorable for CO <sub>2</sub> storage due to their high reactivity and absence of passivation issues
Park and Fan, 2004 [157]	pH swing method for olivine carbonation	Olivine	pH swing method with NaHCO <sub>3</sub> buffer yields rapid olivine carbonation
Chizmeshya et al., 2007 [158]	pH swing method for olivine carbonation	Olivine	NaHCO <sub>3</sub> acts as a catalyst and increases reaction rates of olivine for carbonation
Bearat et al., 2006 [159]	Observation of SiO <sub>2</sub> -rich layer on partially dissolved olivine	Olivine	SiO <sub>2</sub> -rich layer observed on partially dissolved olivine surfaces
Bruni et al., 2002 [160]	Reaction path modeling of olivine carbonation	Olivine	pH of CO <sub>2</sub> -rich fluids reacting with olivine-rich rocks is rapidly buffered to high pH
Eikeland et al., 2015 [161]	Experimental carbonation of olivine	Olivine	Constant rate of olivine carbonation until passiveness occurs
Lewis et al., 2021 [162]	Reaction kinetics of minerals	Various minerals	Plagioclase (Ca/Na rich) and olivine have high reaction rate constant as compared to other trace minerals

### 3. Role of Basalt Geochemistry in CO<sub>2</sub> Storage

The geochemistry of basalt plays a crucial role in the storage of CO<sub>2</sub>, as it possesses natural properties that enable the capture and sequestration of CO<sub>2</sub>. Basalt exhibits a remarkable ability to react with CO<sub>2</sub> and form stable carbonate minerals, a process known as mineral carbonation or carbon sequestration. This phenomenon is highly significant in the context of addressing climate change and reducing greenhouse gas emissions. Basaltic rocks

contain reactive minerals that readily interact with CO<sub>2</sub>, including calcium, magnesium, and iron-bearing minerals. These minerals can undergo dissolution and reprecipitation reactions when exposed to CO<sub>2</sub>, resulting in the transformation of CO<sub>2</sub> into solid carbonate compounds. This process effectively stores the CO<sub>2</sub> over extended periods, providing a means of long-term carbon sequestration.

Water–rock interactions are critical for mineral carbonation to occur. Basalt acts as a host rock, allowing water and dissolved CO<sub>2</sub> to infiltrate its structure. This interaction enables the dissolution of basalt minerals and subsequent precipitation of carbonate minerals. Furthermore, the geochemical composition of basalt is conducive to mineral carbonation. The presence of calcium, magnesium, and iron-bearing minerals in basalt provides the necessary chemical elements for the formation of stable carbonate minerals. The compatibility of basalt's geochemistry with the carbonation process makes it an ideal candidate for CO<sub>2</sub> storage.

The utilization of basalt geochemistry for CO<sub>2</sub> storage involves injecting CO<sub>2</sub> into deep basalt formations, where the natural reactions with the rock can lead to the permanent sequestration of CO<sub>2</sub> in the form of stable carbonate minerals. This approach has gained considerable attention as a potential method for carbon capture and storage, as well as CO<sub>2</sub> removal, offering a promising solution to mitigate greenhouse gas emissions and combat climate change. Various studies have been conducted that discussed the dissolution potential of various basaltic minerals and effect of grain size on CO<sub>2</sub> sequestration as shown in Table 3. The findings of the studies in Table 3 have been further explored in the development of *M.H. reactivity scale* for carbonation reactions in basalt.

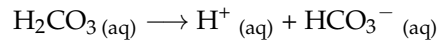
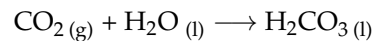
### 3.1. Carbonation Reactions in Basaltic Minerals

In this section, the step-by-step carbonation reactions occurring in basalt for different minerals will be discussed. The carbonation process involves the reaction of CO<sub>2</sub> with minerals present in basalt, leading to the formation of carbonate minerals. The initial steps of CO<sub>2</sub> dissolution are universally observed in all carbonation reactions. However, the subsequent reactions and mineral products can vary depending on the specific minerals present in the basalt. A detailed exploration of the reactions involved in the carbonation of different minerals found in basalt will be provided, shedding light on the transformative process and its significance in carbon sequestration efforts.

#### 3.1.1. Generic Reactions

The first step of CO<sub>2</sub> dissolution is fundamental and occurs universally in all types of minerals found in basalt during the carbonation process. These initial stages lay the foundation for subsequent reactions and mineral transformations. The introduction of CO<sub>2</sub> into basalt formations can be achieved through direct injection or by dissolving it in water prior to injection. This process begins with the dissolution of CO<sub>2</sub> in water, leading to the formation of carbonic acid. The formation of carbonic acid is influenced by various factors, including pressure, temperature, and salinity. As carbonic acid is generated, it alters the pH of the in situ water, enhancing its reactivity. This heightened reactivity prompts the hydrogen ions (H<sup>+</sup>) in the solution to interact with the basalt glass and dissolve the primary minerals present in the rock matrix, liberating cations like calcium (Ca<sup>2+</sup>), magnesium (Mg<sup>2+</sup>), and iron (Fe<sup>2+</sup>) into the solution. This elucidates the pivotal role played by the reactivity of carbonic acid in the process of mineral dissolution and subsequent release of cations during CO<sub>2</sub> injection into basalt formations [14]. These early steps play a crucial role in creating the chemical environment necessary for further interactions and the eventual formation of carbonate minerals [163]. While the subsequent reactions may differ depending on the specific mineral composition of the basalt, these initial two steps provide a common starting point for the carbonation process in all mineral types within basalt [164,165].

### Step 1: CO<sub>2</sub> dissolution



### 3.1.2. Specific Reactions for Minerals

In the subsequent sections, we will delve into the specific carbonation reactions that occur for various minerals found in basalt during the carbonation process. Different minerals within basalt, such as olivine, plagioclase, pyroxene, spinel, and others, exhibit distinct chemical reactions as they undergo carbonation in following steps, which are tabulated in Table 4.

**Table 4.** Carbonation reactions in various basaltic minerals.

Mineral	Weathering (Step 2)	Precipitation (Step 3)	Carbonate Minerals Formation (Step 4)
Olivine [166,167]	$(\text{Mg,Fe})_2\text{SiO}_4(\text{s}) + 4\text{H}^+(\text{aq}) \longrightarrow \text{Mg}^{2+}(\text{aq}) + \text{Fe}^{2+}(\text{aq}) + \text{SiO}_2(\text{s}) + 2\text{H}_2\text{O}(\text{l})$	$\text{Mg}^{2+}(\text{aq}) + 2\text{HCO}_3^-(\text{aq}) \longrightarrow \text{MgCO}_3(\text{s}) + \text{CO}_2(\text{g}) + \text{H}_2\text{O}(\text{l})$	(i) MgCO <sub>3</sub> (magnesite) (ii) (FeCO <sub>3</sub> ) (siderite)
<b>Overall Olivine Carbonation</b>	$(\text{Mg,Fe})_2\text{SiO}_4 + 2\text{CO}_2(\text{g}) + \text{H}_2\text{O}(\text{l}) \rightarrow 2(\text{Mg,Fe})\text{CO}_3(\text{s}) + \text{SiO}_2 \cdot \text{H}_2\text{O}(\text{s})$		
Pyroxene [143,168]	$(\text{Mg,Fe,Ca})(\text{Si,Al})_2\text{O}_6(\text{s}) + 4\text{H}^+(\text{aq}) \longrightarrow 2\text{Mg}^{2+}(\text{aq}) + \text{Fe}^{2+}(\text{aq}) + \text{Ca}^{2+}(\text{aq}) + 2\text{Al}^{3+}(\text{s}) + 4\text{SiO}_2(\text{s}) + 4\text{H}_2\text{O}(\text{l})$	$\text{Mg}^{2+}(\text{aq}) + 2\text{HCO}_3^-(\text{aq}) \longrightarrow \text{MgCO}_3(\text{s}) + \text{CO}_2(\text{g}) + \text{H}_2\text{O}(\text{l})$ $\text{Fe}^{2+}(\text{aq}) + 2\text{HCO}_3^-(\text{aq}) \longrightarrow \text{FeCO}_3(\text{s}) + \text{CO}_2(\text{g}) + \text{H}_2\text{O}(\text{l})$ $\text{Ca}^{2+}(\text{aq}) + 2\text{HCO}_3^-(\text{aq}) \longrightarrow \text{CaCO}_3(\text{s}) + \text{CO}_2(\text{g}) + \text{H}_2\text{O}(\text{l})$	MgCO <sub>3</sub> (magnesite), FeCO <sub>3</sub> (siderite), and CaCO <sub>3</sub> (calcite)
<b>Overall Pyroxene Carbonation</b>	$3(\text{Mg,Fe,Ca})(\text{Si,Al})_2\text{O}_6(\text{s}) + 3\text{CO}_2(\text{g}) + 8\text{H}_2\text{O}(\text{l}) \rightarrow 3(\text{Mg,Fe,Ca})\text{CO}_3 + \text{Al}_2\text{O}_3 \cdot 2\text{H}_2\text{O}(\text{s}) + 6\text{SiO}_2 \cdot \text{H}_2\text{O}(\text{s})$		
Plagioclase [56]	$(\text{Na,Ca})(\text{Al,Si})\text{AlSi}_2\text{O}_8(\text{s}) + 4\text{H}^+(\text{aq}) \longrightarrow \text{Ca}^{2+}(\text{aq}) + \text{Na}^+(\text{aq}) + 2\text{Al}^{3+}(\text{s}) + 4\text{SiO}_2(\text{s}) + 4\text{H}_2\text{O}(\text{l})$	$\text{Ca}^{2+}(\text{aq}) + 2\text{HCO}_3^-(\text{aq}) \longrightarrow \text{CaCO}_3(\text{s}) + \text{CO}_2(\text{g}) + \text{H}_2\text{O}(\text{l})$ $\text{Na}^+(\text{aq}) + 2\text{HCO}_3^-(\text{aq}) \longrightarrow \text{NaHCO}_3(\text{aq}) + \text{CO}_2(\text{g})$	CaCO <sub>3</sub> (calcite) and NaHCO <sub>3</sub> (sodium bicarbonate)
<b>* Overall Plagioclase Carbonation</b>	$(\text{Na,Ca})(\text{Al,Si})\text{AlSi}_2\text{O}_8(\text{s}) + \text{CO}_2(\text{g}) + \text{H}_2\text{O}(\text{l}) \longrightarrow \text{CaCO}_3(\text{s}) + \text{NaHCO}_3(\text{aq}) + \text{Al}_2\text{O}_3 \cdot \text{H}_2\text{O}(\text{s}) + \text{SiO}_2(\text{s})$		

\* Stoichiometric coefficients are not provided since plagioclase has repeating units on the reactant side.

### Step 2: Weathering of Minerals (Dissolution)

During the carbonation process, the minerals present in basalt undergo weathering, leading to their dissolution. This step involves the interaction between the mineral surface and the surrounding solution, resulting in the release of metal ions and the formation of silicate species. The specific reactions vary depending on the mineral type.

### Step 3: Reaction between Metal Ions and Bicarbonate

In this step, the metal ions released during the weathering process react with bicarbonate ions present in the solution. These reactions contribute to the overall carbonation process by forming carbonate minerals.

### Step 4: Formation of Carbonate Minerals

In this step, the carbonate minerals precipitate from the solution as a result of the reactions between metal ions and bicarbonate ions. The specific carbonate minerals formed depend on the availability of metal ions and the prevailing conditions.

### 3.2. Factors Affecting Reactivity of Basaltic Minerals in Different Basalts

In this section, we will delve into the factors that influence the reactivity of basaltic minerals and their carbonation potential. The reactivity of these minerals can vary depending on several factors, including the specific composition and type of basalt.

#### 3.2.1. Alkaline Basalt

CO<sub>2</sub> storage in alkaline basalt is particularly influenced by the mineralogy of the rock and specific factors that impact mineral reactivity. Alkaline basalts is characterized by the presence of minerals such as plagioclase feldspar, clinopyroxene, and olivine, which play a crucial role in the carbon sequestration process. Plagioclase, a key mineral in alkaline basalts, exhibits high reactivity and can rapidly react with CO<sub>2</sub> to form stable carbonate minerals [169,170]. Olivine and clinopyroxene also contribute to the overall reactivity, although their carbonation rates may vary and require specific conditions or longer reaction times.

The mineralization reactions involved in CO<sub>2</sub> storage for alkaline basalts primarily include the dissolution of minerals and the subsequent precipitation of carbonate minerals. Dominant minerals are olivine and pyroxene and the key mineralization reactions that occur during the carbonation process are tabulated in Table 4.

The dissolved calcium ions and bicarbonate ions react to form calcium carbonate (CaCO<sub>3</sub>), water (H<sub>2</sub>O), and release CO<sub>2</sub>. These mineralization reactions involve the transformation of CO<sub>2</sub> into stable carbonate minerals, effectively sequestering CO<sub>2</sub> in a solid form within the alkaline basalt formations. It is important to note that the reactions mentioned above are simplified representations of the complex processes occurring during mineral carbonation. The actual reactions and reaction rates can be influenced by various factors, including temperature, pressure, fluid composition, and the specific mineralogy of the alkaline basalts [171].

Several factors influence the reactivity of minerals in alkaline basalts and, consequently, the efficiency of CO<sub>2</sub> storage. Here are some specific values and considerations for these factors:

**Temperature and Pressure:** The reactivity of minerals in alkaline basalts increases with higher temperatures. Typically, mineral carbonation reactions occur more rapidly at elevated temperatures. Optimal temperatures for efficient carbonation of olivine range from 150 to 300 degrees Celsius [172]. Mostly, alkaline basalts are present in the upper layer of the Earth's crust so it can undergo carbonation at atmospheric pressure, i.e., 1 atm. However, the basalt located deep in the Earth's crust or in the subduction zone may undergo carbonation at higher pressures ranging to a few hundred MPa. However, extreme pressures can affect the mineralogical composition and physical properties of basalt, potentially impacting reactivity [173].

**Dissolution Rate:** Alkali basalt contains 30-45% plagioclase, and plagioclase have the highest dissolution rates as depicted in Table 2 compared to olivine and pyroxene.

**Fluid Composition:** The composition of fluids interacting with alkaline basalts affects mineral reactivity. Fluids rich in dissolved CO<sub>2</sub> and alkaline ions, such as calcium and magnesium, enhance mineral dissolution and the subsequent precipitation of carbonate minerals [174].

**Fluid pH and Redox Conditions:** The pH of the fluid is a crucial factor in mineral reactivity. In the case of alkaline basalts, slightly alkaline to neutral pH conditions (pH 7 to 9) generally favor mineral carbonation. Redox conditions, such as the presence of oxidizing or reducing agents, can influence the stability and reactivity of minerals but are typically controlled within a range suitable for carbonation [175].

**Grain Size and Surface Area:** Alkali basalt have dominant percentage of plagioclase. According to Table 2, plagioclase demonstrates high reactivity due to its smaller grain size and larger surface area, making it particularly favorable for carbonation processes.

**Rock Composition:** The specific mineralogical composition of alkaline basalts affects its reactivity. Basalts rich in olivine minerals, with a higher olivine content and reactive mineral pyroxene, generally exhibit greater reactivity and higher carbon storage potential [176].

**Geological Setting:** The geological setting influences the availability of fluids and other factors that impact mineral reactivity. Basaltic formations in hydrothermal areas or areas with enhanced fluid circulation are more favorable for mineral carbonation reaction [177].

### 3.2.2. Tholeiitic Basalt

The mineralization reactions that occur in tholeiitic basalts during CO<sub>2</sub> storage involve the dissolution of certain minerals and the subsequent precipitation of carbonate minerals. Here are the detailed mineralization reactions that occur:

Tholeiitic basalts typically contain minerals such as plagioclase feldspar, pyroxene (including augite and pigeonite), magnetite, and sometimes olivine. These minerals play a significant role in the carbon sequestration process. The reactivity of minerals in tholeiitic basalt determines their ability to undergo mineral carbonation reactions with CO<sub>2</sub>. Olivine and pyroxene minerals are generally more reactive compared to plagioclase feldspar. Magnetite can also contribute to carbonation reactions but to a lesser extent. The key mineralization reactions that occur during the carbonation process are tabulated in Table 4:

The factors that influence the reactivity of minerals in tholeiitic basalt and, consequently, the efficiency of CO<sub>2</sub> storage are as follows:

**Temperature and Pressure:** Higher temperatures generally increase the rate of mineral carbonation reactions. Elevated temperatures can enhance the kinetic rates of reactions, promoting the conversion of CO<sub>2</sub> into carbonate minerals. The optimal temperature range for efficient carbonation of minerals in tholeiitic basalts typically falls between 100 and 200 degrees Celsius [178]. Pressure conditions can impact the stability and reactivity of minerals. High-pressure environments may favor mineral carbonation reactions by promoting closer contact between minerals and CO<sub>2</sub>. However, depending upon the geological settings (mid-ocean ridges, continental flood basalts, and rift zones), the carbonation pressure may vary in tholeiitic basalts. In the case of tholeiitic basalts, pressure conditions ranging from atmospheric pressure to a few hundred megapascals (MPa) are commonly encountered [179].

**Dissolution Rate:** Tholeiitic basalt contains 40%–70% plagioclase and plagioclase has the highest dissolution rates as depicted in Table 2 compared to Olivine and Pyroxene. Thus, tholeiitic basalt has higher carbonation potential than alkali basalts.

**Fluid Composition:** The composition of fluids in contact with tholeiitic basalts affects mineral reactivity. Fluids can introduce dissolved CO<sub>2</sub> and other ions that participate in carbonation reactions. The presence of certain ions, such as calcium, magnesium, and iron, can enhance mineral dissolution and precipitation, leading to effective CO<sub>2</sub> storage [180].

**Fluid pH and Redox Conditions:** The pH and redox conditions of the fluid significantly impact mineral reactivity. Different minerals have specific pH ranges at which they are more prone to dissolution or precipitation. Tholeiitic basalts generally exhibit slightly acidic to neutral pH conditions (pH 5 to 7) favorable for mineral carbonation. Redox conditions can affect the stability of minerals and their ability to react with CO<sub>2</sub> [181].

**Grain Size and Surface Area:** It has dominant percentage of plagioclase. According to Table 2, plagioclase demonstrates high reactivity due to its smaller grain size and larger surface area, making it particularly favorable for carbonation process.

**Rock Composition:** The specific mineralogical composition of tholeiitic basalt affects its reactivity. Basalts rich in olivine and pyroxene minerals tend to exhibit higher reactivity due to the presence of highly reactive phases. The relative abundance and distribution of these minerals within the tholeiitic basalt can influence the overall carbonation potential [182].

**Geological Setting:** The geological setting in which tholeiitic basalt is located can also impact its reactivity for CO<sub>2</sub> storage. Factors such as the availability of fluids, hydrothermal

activity, and the presence of other minerals or rock types can influence the effectiveness of mineral carbonation processes [182].

Considering these factors, CO<sub>2</sub> storage in tholeiitic basalts can be optimized by controlling temperature, pressure, fluid composition, pH, and redox conditions. Proper selection of basaltic rocks with favorable mineralogy and considering the geological setting can enhance the reactivity and carbon storage potential of tholeiitic basalt formations.

### 3.2.3. Transitional Basalts

CO<sub>2</sub> storage in transition basalts is influenced by the reactivity of its minerals and various factors that affect mineral reactivity. Transition basalts typically contain minerals such as plagioclase feldspar, pyroxene (including augite and pigeonite), olivine, and magnetite. These minerals play a crucial role in the carbon sequestration process. The reactivity of minerals in transition basalts determines their ability to undergo mineral carbonation reactions with CO<sub>2</sub>. Olivine and pyroxene minerals are generally more reactive compared to plagioclase feldspar. Magnetite can also contribute to carbonation reactions but to a lesser extent.

The mineralization reactions involved in CO<sub>2</sub> storage in transition basalts include the dissolution of certain minerals and the subsequent precipitation of carbonate minerals. The key mineralization reactions that occur during the carbonation process are tabulated in Table 4. The following factors influence the reactivity of minerals in transition basalts and, consequently, the efficiency of CO<sub>2</sub> storage:

**Temperature and Pressure:** Higher temperatures generally increase the rate of mineral carbonation reactions. Elevated temperatures enhance the kinetic rates of reactions, promoting the conversion of CO<sub>2</sub> into carbonate minerals. The optimal temperature range for efficient carbonation of minerals in transition basalts typically falls between 100 and 200 degrees Celsius [183]. Pressure conditions can impact the stability and reactivity of minerals. High-pressure environments may favor mineral carbonation reactions by promoting closer contact between minerals and CO<sub>2</sub>. In the case of transition basalts, pressure conditions ranging from atmospheric pressure to a few hundred megapascals (MPa) are commonly encountered [184].

**Dissolution Rate:** Transition basalt contains 30%–50% plagioclase and plagioclase has the highest dissolution rates as depicted in Table 2 compared to Olivine and Pyroxene. Thus, these basalts have carbonation potential ranging between alkali and tholeiitic basalts.

**Fluid Composition:** The composition of fluids in contact with transition basalts affects their mineral reactivity. Fluids can introduce dissolved CO<sub>2</sub> and other ions that participate in carbonation reactions. The presence of certain ions, such as calcium, magnesium, and iron, can enhance mineral dissolution and precipitation, leading to effective CO<sub>2</sub> storage [185].

**Fluid pH and Redox Conditions:** The pH and redox conditions of the fluid significantly impact mineral reactivity. Different minerals have specific pH ranges at which they are more prone to dissolution or precipitation. Transition basalts generally exhibit slightly acidic to neutral pH conditions (pH 5 to 7), which are favorable for mineral carbonation. Redox conditions can affect the stability of minerals and their ability to react with CO<sub>2</sub> [186].

**Grain Size and Surface Area:** It has a dominant percentage of plagioclase. According to Table 2, plagioclase demonstrates high reactivity due to its smaller grain size and larger surface area, making it particularly favorable for carbonation process.

**Rock Composition:** The specific mineralogical composition of transition basalts affects their reactivity. Basalts rich in olivine and pyroxene minerals tend to exhibit higher reactivity due to the presence of highly reactive phases. The relative abundance and distribution of these minerals within the transition basalt can influence the overall carbonation potential [187].

**Geological Setting:** The geological setting in which transition basalts are located can also impact their reactivity for CO<sub>2</sub> storage. Factors such as the availability of fluids,

hydrothermal activity, and the presence of other minerals or rock types can influence the effectiveness of mineral carbonation processes [188].

#### 3.2.4. High-Magnesium Basalts (HMB)

The mineralization reactions that occur in high-magnesium basalts (HMB) during CO<sub>2</sub> storage are primarily driven by the reactivity of minerals present in the rock. The major minerals in HMB include olivine, pyroxene (augite and pigeonite), plagioclase feldspar, and magnetite. These minerals undergo chemical transformations as they react with CO<sub>2</sub>, leading to the formation of carbonate minerals. The mineralization reactions specific to HMB are tabulated in Table 4. CO<sub>2</sub> storage in high-magnesium basalts (HMB) is influenced by several factors that affect the reactivity of minerals and, subsequently, the efficiency of carbon sequestration. These factors specific to HMB include:

**Temperature and Pressure:** The temperature range for optimal carbonation in HMB typically falls between 150 to 350 degrees Celsius. Higher temperatures generally enhance the rates of mineral carbonation reactions, facilitating the conversion of CO<sub>2</sub> into carbonate minerals [189]. Pressure conditions encountered in HMB usually range from atmospheric pressure to a few hundred megapascals (MPa). Pressure can influence mineral stability and enhance the contact between minerals and CO<sub>2</sub>, promoting carbonation reactions [190].

**Dissolution Rate:** HMB contains dominant percentage of olivine that has lower dissolution rates as depicted in Table 2 compared to Plagioclase and Pyroxene. Thus, HMB will have lower carbonation potential as compared to above-mentioned basalts.

**Fluid Composition:** The composition of fluids interacting with HMB affects mineral reactivity. Fluids can introduce dissolved CO<sub>2</sub> and other ions that participate in carbonation reactions. Ions such as calcium, magnesium, and iron can enhance mineral dissolution and precipitation, increasing CO<sub>2</sub> storage capacity [191].

**Fluid pH and Redox Conditions:** HMB typically exhibits slightly acidic to neutral pH conditions (pH 5 to 7), which are favorable for mineral carbonation. Redox conditions can influence mineral stability and their ability to react with CO<sub>2</sub> [192].

**Grain Size and Surface Area:** It has dominant percentage of olivine. According to Table 2, olivine demonstrates moderate reactivity due to its moderate grain size and moderate surface area, making it moderately favorable for carbonation process.

**Rock Composition:** The mineralogical composition of HMB, with high concentrations of olivine and pyroxene, contributes to its reactivity. Basalts rich in these minerals tend to exhibit higher carbonation potential due to their highly reactive nature [193].

**Geological Setting:** The geological setting in which HMB is located can impact its reactivity for CO<sub>2</sub> storage. Factors such as the availability of fluids, hydrothermal activity, and the presence of other minerals or rock types can influence the effectiveness of mineral carbonation processes [193].

#### 3.2.5. Calc-Alkaline Basalts

The mineralization reactions that occur in calc-alkaline basalts during CO<sub>2</sub> storage involve the reactivity of specific minerals present in the rock. The major minerals in Calc-alkaline basalts, including plagioclase feldspar, pyroxene (augite and pigeonite), amphibole, and occasionally olivine, undergo chemical transformations as they react with CO<sub>2</sub>, resulting in the formation of carbonate minerals. The mineralization reactions specific to calc-alkaline basalts are tabulated in Table 4. These mineralization reactions contribute to the storage of CO<sub>2</sub> in calc-alkaline basalts by converting CO<sub>2</sub> into stable carbonate minerals. The extent of mineral carbonation depends on factors such as temperature, pressure, fluid composition, pH, redox conditions, time, and the specific mineralogy of the rock. By optimizing these conditions, the efficiency of CO<sub>2</sub> storage in calc-alkaline basalts can be improved, offering a promising avenue for carbon sequestration and climate change mitigation.

The minerals commonly found in calc-alkaline basalts include plagioclase feldspar, pyroxene (augite and pigeonite), amphibole, and sometimes olivine. These minerals exhibit

different degrees of reactivity and contribute to the carbonation reactions. The specific factors that affect their reactivity and, consequently, CO<sub>2</sub> storage efficiency in calc-alkaline basalts are as follows:

**Temperature and Pressure:** The temperature range for optimal carbonation in calc-alkaline basalts typically falls between 150 to 350 degrees Celsius. Higher temperatures generally enhance the rates of mineral carbonation reactions, promoting the conversion of CO<sub>2</sub> into carbonate minerals [194]. Pressure conditions encountered in calc-alkaline basalts usually range from atmospheric pressure to a few hundred megapascals (MPa). Pressure affects mineral stability and influences the availability of fluids and reactants, influencing the carbonation reactions [195].

**Dissolution Rate:** Calc-alkaline basalt contains 10%–40% plagioclase, which is relatively low. Though plagioclase has higher dissolution rates as depicted in Table 2 compared to olivine and pyroxene, but in context of dissolution rates, its carbonation potential will be the lowest among alkali, tholeiitic, and transition basalts.

**Fluid Composition:** The composition of fluids interacting with calc-alkaline basalts affects mineral reactivity. Fluids can introduce dissolved CO<sub>2</sub> and other ions that participate in carbonation reactions. The presence of calcium, magnesium, and iron ions can enhance mineral dissolution and precipitation, increasing CO<sub>2</sub> storage capacity [196].

**Fluid pH and Redox Conditions:** Calc-alkaline basalts typically exhibit slightly acidic to neutral pH conditions (pH 5 to 7), which favor mineral carbonation. Redox conditions can also influence mineral stability and their ability to react with CO<sub>2</sub> [197].

**Grain Size and Surface Area:** It has a dominant percentage of plagioclase. According to Table 2, plagioclase demonstrates high reactivity due to its smaller grain size and larger surface area, making it particularly favorable for the carbonation process.

**Rock Composition:** The mineralogical composition of calc-alkaline basalts, with plagioclase feldspar, pyroxene, amphibole, and occasionally olivine, contributes to their reactivity. The proportions and reactivity of these minerals affect the overall carbonation potential of the rock [198].

**Geological Setting:** The geological setting in which calc-alkaline basalts are found can influence their reactivity for CO<sub>2</sub> storage. Factors such as the presence of other minerals or rock types, hydrothermal activity, and fluid availability can affect the effectiveness of mineral carbonation processes [199].

### 3.2.6. Ocean Island Basalts (OIB)

Ocean island basalts (OIBs) have specific mineral compositions that play a vital role in the carbonation process during CO<sub>2</sub> storage. The reactivity of minerals such as plagioclase feldspar, pyroxene, olivine, and occasionally amphibole in OIBs allows them to undergo chemical transformations when exposed to CO<sub>2</sub>, resulting in the formation of stable carbonate minerals. These mineralization reactions are crucial for sequestering CO<sub>2</sub> in basalt, offering a potential solution for climate change mitigation.

**Temperature and Pressure:** Several factors influence the efficiency of carbon sequestration in OIBs. Temperature is a significant factor, as the optimal range for carbonation in OIBs typically falls between 150 to 350 degrees Celsius. Higher temperatures promote faster rates of mineral carbonation reactions, facilitating the conversion of CO<sub>2</sub> into carbonate minerals [200]. Pressure conditions encountered in OIBs range from atmospheric pressure to a few hundred megapascals (MPa). Pressure affects the stability of minerals and influences the availability of fluids and reactants, thereby impacting the carbonation reactions [201].

**Dissolution Rate:** OIB contains olivine (40%–50%) as a dominant mineral that has lower dissolution rates as depicted in Table 2 compared to plagioclase and pyroxene. Thus, OIB will have lower carbonation potential as compared to alkali, tholeiitic, and transition basalt.

**Fluid Composition:** The composition of fluids interacting with OIBs also influences mineral reactivity. Fluids introduce dissolved CO<sub>2</sub> and other ions that participate in

carbonation reactions. Calcium, magnesium, and iron ions, in particular, can enhance mineral dissolution and precipitation, increasing the capacity for CO<sub>2</sub> storage [202].

**pH and Redox Reactions:** Fluid pH and redox conditions play a role in OIBs, with slightly acidic to neutral pH conditions (pH 5 to 7) favoring mineral carbonation. Redox conditions can also influence mineral stability and their ability to react with CO<sub>2</sub> [203].

**Grain Size and Surface Area:** It has a dominant percentage of olivine. According to Table 2, olivine demonstrates moderate reactivity due to its moderate grain size and moderate surface area, making it moderately favorable for carbonation process.

**Rock Composition:** The specific mineralogy and proportions of minerals in OIBs impact their reactivity and CO<sub>2</sub> storage potential. Certain minerals, such as olivine, exhibit higher reactivity to carbonation, significantly influencing the overall CO<sub>2</sub> storage capacity [204].

**Geological Setting:** The geological setting of ocean island basalts (OIBs) significantly impacts the efficiency of CO<sub>2</sub> storage. Factors such as rock permeability, porosity, fractures, fault networks, water–rock interactions, geological heterogeneity, and depth/pressure conditions influence the availability of reactants, fluid flow, mineral reactivity, and the overall carbon sequestration potential. Understanding and characterizing these geological aspects are crucial for optimizing CO<sub>2</sub> storage strategies in OIBs and ensuring long-term stability [204].

### 3.2.7. Island Arc Basalts (IAB)

CO<sub>2</sub> storage in island arc basalts (IAB) involves the reactivity of its minerals and is influenced by various factors that affect the efficiency of carbon sequestration. Island arc basalts are formed in subduction zones where oceanic plates are being subducted beneath continental plates, leading to the formation of volcanic arcs. The mineralogy and specific characteristics of island arc basalts influence their potential for CO<sub>2</sub> storage.

The mineralization reactions involved in CO<sub>2</sub> storage in island arc basalts (IAB) primarily depend on the reactivity of the minerals present in the rock. The specific reactions can vary based on the mineralogy and composition of the basalts. However, Table 4 contains general mineralization reactions that may occur during CO<sub>2</sub> storage in island arc basalts:

**Temperature and Pressure:** The temperature range for optimal carbonation in island arc basalts varies, typically ranging from 200 to 500 degrees Celsius. Higher temperatures enhance the rate of mineral carbonation reactions [205]. Island arc basalts experience moderate- to high-pressure conditions due to the subduction process. The pressure range encountered can vary from several hundred megapascals (MPa) to gigapascals (GPa). Pressure affects mineral stability and the availability of reactants, impacting carbonation reactions [206].

**Dissolution Rate:** OIB has high percentage of plagioclase (30%–60%) that has the highest dissolution rates as depicted in Table 2 compared to Olivine and Pyroxene. Thus, OIB will have lower carbonation potential as compared to above-mentioned basalts but lower than tholeiitic basalt in context of dissolution rates.

**Fluid Composition:** The composition of fluids interacting with island arc basalts influences mineral reactivity and carbonation processes. The presence of water-rich fluids with dissolved CO<sub>2</sub> and other ions enhances mineral dissolution and precipitation, facilitating carbon storage [207].

**Fluid pH and Redox Conditions:** Island arc basalts typically experience slightly acidic to neutral pH conditions (pH 5 to 7), which can promote mineral carbonation. Redox conditions, including the presence of oxidizing or reducing agents, influence mineral stability and reactivity [208].

**Grain Size and Surface Area:** It has dominant percentage of plagioclase. According to Table 2, plagioclase demonstrates high reactivity due to its smaller grain size and larger surface area, making it particularly favorable for carbonation process.

**Rock Composition:** The specific mineralogy and proportions of minerals in island arc basalts affect their reactivity and carbonation potential. The presence of reactive minerals, such as olivine or pyroxene, can significantly contribute to CO<sub>2</sub> storage [209].

Considering the mineralogy of island arc basalts and optimizing temperature, pressure, fluid composition, pH, redox conditions, time, and rock composition, the efficiency of CO<sub>2</sub> storage can be enhanced. Carbonation reactions convert CO<sub>2</sub> into stable carbonate minerals, effectively sequestering CO<sub>2</sub> from the atmosphere. Island arc basalts provide a potential reservoir for CO<sub>2</sub> storage, contributing to climate change mitigation efforts.

A summary of the above discussion related to the parameters affecting reactivity of basalt for its carbonation potential is given in Table 5.

**Table 5.** Summary of parameters affecting reactivity of basaltic minerals for favorable carbonation reactions in various basalt types.

Basalt Type	T Range (°C)	P Range	Mineralogy	Fluid Composition	Grain Size (Avg)	Primary Reaction	Geological Setting
Alkaline Basalts	130–150	1 atm to few hundred MPa	Plagioclase, Pyroxene	CO <sub>2</sub> -rich fluid	Bigger grain size and smaller surface area	Mineral carbonation (Ca-bearing silicates)	Continental rift zones
Tholeiitic Basalt	100–200	1 atm to few hundred MPa	Plagioclase, Pyroxene, Olivine	CO <sub>2</sub> -rich fluid	Bigger grain size and smaller surface area	Mineral carbonation (Ca-bearing silicates)	Mid-oceanic ridges
Transition Basalt	100–200	1 atm to few hundred MPa	Plagioclase, Pyroxene, Olivine	CO <sub>2</sub> -rich fluid	Bigger grain size and smaller surface area	Mineral carbonation (Ca-bearing silicates)	Transitional tectonic settings
High-Magnesium Basalt	150–300	1 atm to few hundred MPa	Olivine, Pyroxene	CO <sub>2</sub> -rich fluid	Smaller grain size and smaller surface area	Mineral carbonation (Mg-bearing silicates)	Hotspot volcanic regions
Calc-alkaline Basalt	150–300	1 atm to few hundred MPa	Plagioclase, Pyroxene	CO <sub>2</sub> -rich fluid	Bigger grain size and smaller surface area	Mineral carbonation (Ca-bearing silicates)	Subduction zones
Ocean Island Basalt	150–350	1 atm to few hundred MPa	Plagioclase, Pyroxene, Olivine	CO <sub>2</sub> -rich fluid	Smaller grain size and smaller surface area	Mineral carbonation (Ca-bearing silicates)	Hotspot volcanism
Island Arc Basalt	200–500	Hundreds of MPa	Plagioclase, Pyroxene, Amphibole	CO <sub>2</sub> -rich fluid	Bigger grain size and smaller surface area	Mineral carbonation (Ca-bearing silicates)	Volcanic arc settings

#### 4. Formulation of a *M.H. reactivity scale* for Mineralization Process in Seven Basalt Types

Table 6 presents a critical analysis of mineral reactivity in form an *M.H. reactivity scale* for carbonation reactions and CO<sub>2</sub> storage potential across different basalt types. The *M.H. reactivity scale* consists of two aspects. The first aspect is the direct indicator of reactivity, which are the grain size and dissolution rate. The remaining factors represent the favorable conditions under which mineralization reactions will occur in these types of basalts. In alkaline basalts, the moderate to high reactivity scale (4) indicates a moderate to high potential for carbonation. The dominant mineral, plagioclase feldspar (30%–45%), can participate in mineralization reactions, suggesting its role in CO<sub>2</sub> storage. Tholeiitic

basalt, with a high reactivity scale (4), exhibits a relatively high potential for carbonation. The presence of plagioclase as the reactive mineral with higher percentage highlights its contribution to efficient mineralization processes, thus enhancing CO<sub>2</sub> storage capabilities. Transition basalt, with a moderate to high reactivity scale (4.5), shows promising potential for carbonation. The dominant minerals, plagioclase (30%–50%) and reactive minerals such as clinopyroxene and spinel, contribute significantly to the mineralization reactions, indicating favorable CO<sub>2</sub> storage prospects. High-magnesium basalt, scoring a moderate reactivity scale (3), demonstrates moderate potential for carbonation reactions. The second reactive mineral, olivine (30%–60%), exhibits lower reactivity with CO<sub>2</sub> as compared to plagioclase, further enhancing the mineralization process and CO<sub>2</sub> storage capacity. Calc-alkaline basalt, with a low–moderate reactivity scale (2.5), shows a moderate potential for carbonation. Plagioclase feldspar (10%–40%) as the dominant mineral, along with reactive minerals like feldspathoids and olivine, contributes to the overall reactivity, suggesting a role in CO<sub>2</sub> storage. Similarly, for OIC which gets a rating of 2.5 due to absence of plagioclase as a dominant mineral but it still has olivine, which has higher surface area. Lastly, IAB containing high percentage of plagioclase gets a 4.5 rating. These critical analyses provide valuable insights into the reactivity of minerals in each basalt type, offering guidance for effective CO<sub>2</sub> sequestration strategies and carbon storage potential. However, it is crucial to mention here that *M.H. reactivity scale* gives the qualitative information about the carbonation potential of the different types of basalts based upon reactive and dominant minerals present in respective basalt types. The less reactive and minerals in low percentage will also contribute to overall carbonation potential of these basalts. Therefore, it is worth mentioning here that this scale is not an absolute scale but mere a qualitative relative scale where carbonation potential of different basalt types can be compared and visualized based upon specific factors.

**Table 6.** *M.H. reactivity scale* rating reactivity of basaltic dominant and reactive minerals for carbonation reactions.

Basalt Type	Dominant Mineral Composition (%)	Reactive Mineral	Dissolution Rate	Surface Area	Reactivity Scale
Alkaline Basalts	Plagioclase Feldspar (30%–45%)	Plagioclase	High	Low	4 (Moderate to High)
Tholeiitic Basalt	Plagioclase Feldspar (40%–70%)	Plagioclase	High	Low	5 (High)
Transition Basalt	Plagioclase (30%–50%)	Plagioclase	High	Low	4.5 (Moderate to High)
High-Magnesium Basalt	Olivine (30%–60%)	Olivine	Low	High	3 (Moderate)
Calc-alkaline Basalt	Plagioclase Feldspar (10%–40%)	Plagioclase Olivine	High	Low	2.5 (Low to Moderate)
Ocean Island Basalt (OIB)	Olivine (40%–50%)	Olivine	Low	High	2.5 (Low to Moderate)
Island Arc Basalt	Plagioclase Feldspar (30%–60%)	Plagioclase	High	Low	4.5 (Moderate to High)

#### *Influence of Basalt Geochemistry on CO<sub>2</sub> Capillary Trapping and Retention*

Basalt geochemistry plays a vital role in the process of capillary trapping, a fundamental mechanism for the geological storage of CO<sub>2</sub> within basalt formations. Capillary trapping involves the physical confinement of CO<sub>2</sub> in the capillary spaces between mineral grains or fluid interfaces due to capillary forces. Basalt's geochemical characteristics have a direct impact on this process. [210]. The distribution of pore sizes within basalt formations is influenced by their mineral composition, and this affects the effectiveness of capillary

trapping. Basalts typically possess a variety of pore sizes, including small capillary pores, which are crucial for capillary forces to come into play and retain CO<sub>2</sub>. Additionally, the wettability of mineral surfaces within basalt determines the interaction between CO<sub>2</sub> and the rock. If CO<sub>2</sub> is less wetting than the resident fluids, it can be preferentially trapped in capillary spaces due to capillary pressure differences. [211,212].

The interfacial tension between CO<sub>2</sub> and fluids present in the formation also affects capillary trapping. Basalt's geochemical composition can influence this interfacial tension, further impacting the capillary forces responsible for retaining CO<sub>2</sub>. Moreover, the surface properties of basalt, such as mineral coatings and roughness, influence the interaction between CO<sub>2</sub> and solid surfaces, which, in turn, affects the distribution and entrapment of CO<sub>2</sub> within the pore spaces. [213]. Basalt's geochemical properties not only facilitate initial capillary trapping but also contribute to the long-term stability of stored CO<sub>2</sub>. Mineral reactions triggered by the presence of CO<sub>2</sub> can lead to changes in pore structure, mineral precipitation, and even mineralization over time. These reactions can enhance the permanence of capillary trapping by altering the rock matrix and further immobilizing CO<sub>2</sub>. [20,214].

In summary, the geochemical characteristics of basalt, encompassing pore structure, wettability, interfacial tension, and surface properties, collectively dictate the extent and efficiency of capillary trapping of CO<sub>2</sub>. The intricate interplay of these factors creates an environment conducive to physically confining CO<sub>2</sub> within the rock matrix for long periods, which is crucial for ensuring the stability and permanence of geological carbon storage efforts. Understanding and leveraging basalt's geochemistry in the context of capillary trapping contribute to the development of effective carbon capture and storage strategies. [215,216].

## 5. Challenges in Understanding Basalt Geochemistry for CO<sub>2</sub> Storage

The study of basalt geochemistry for CO<sub>2</sub> storage presents several challenges and uncertainties that need to be addressed in order to fully understand and optimize the potential of basalt formations as CO<sub>2</sub> storage sites. These challenges arise from the complex nature of basalt geochemistry and the dynamic processes involved in CO<sub>2</sub> storage [217]. Basalt formations display significant variations in terms of their mineral composition, porosity, permeability, and interactions with water and rocks [218]. These differences, known as heterogeneity, play a crucial role in accurately predicting how CO<sub>2</sub> behaves within the reservoir. The geochemical makeup of basalt can impact the rates at which minerals dissolve, carbonate minerals precipitate, and CO<sub>2</sub> is efficiently trapped [219]. One important aspect that remains poorly quantified is the reactive surface area of basalt rocks. This surface area influences the speed at which minerals dissolve and carbonation reactions occur [220,221]. To measure the reactive surface area, advanced techniques like electron microscopy are required to capture the micro-scale features of the rocks. The lack of precise measurements introduces uncertainties when estimating the storage capacities of CO<sub>2</sub> and predicting reaction kinetics [14,222].

The kinetics of mineral dissolution and carbonation reactions in basalt formations are not yet fully understood. The rates at which minerals react with CO<sub>2</sub> and water depend on various factors, including temperature, pressure, mineralogy, and water chemistry [223]. A better understanding of these reaction kinetics is essential for optimizing injection strategies and accurately predicting the long-term stability of CO<sub>2</sub> storage. Although numerous studies have examined basalt geochemistry and CO<sub>2</sub> storage at laboratory or small-scale field sites, scaling up these findings to larger, real-world basalt formations presents challenges [224]. Complex interactions between CO<sub>2</sub>, water, and rock occur at different spatial and temporal scales. Bridging the gap between laboratory experiments and field-scale applications requires extensive research and validation [225].

Assessing the long-term stability of CO<sub>2</sub> storage and the potential for leakage pathways in basalt formations is a critical challenge [226]. Monitoring techniques must be developed to accurately detect and quantify the migration and fate of CO<sub>2</sub> within the

reservoir over extended periods. Understanding the potential risks associated with CO<sub>2</sub> leakage, such as through fractures or faults in the basalt, is crucial for ensuring the effectiveness and safety of CO<sub>2</sub> storage. Basalt formations can contain complex geological features like faults, fractures, and volcanic intrusions, which can impact fluid flow pathways, rock permeability, and the stability of CO<sub>2</sub> storage [52]. Precisely characterizing these geological uncertainties and their influence on basalt geochemistry is essential for reliable CO<sub>2</sub> storage assessments [227].

Addressing these challenges and uncertainties requires collaborative research efforts involving experts from geology, geochemistry, hydrology, and engineering. Advancements in laboratory experimentation, modeling techniques, and field-scale demonstrations are necessary to improve our understanding of basalt geochemistry for CO<sub>2</sub> storage [228]. By overcoming these obstacles, we can fully utilize the potential of basalt formations as a viable and effective option for CO<sub>2</sub> storage, thus contributing to global efforts in mitigating climate change. The process of mineralizing basalt for CO<sub>2</sub> storage involves complex geochemical reactions that introduce uncertainties and challenges. These uncertainties arise due to the intricate nature of the reactions and our limited understanding of certain factors that influence mineralization [229]. The reactivity of minerals in basalt formations towards CO<sub>2</sub> is not well-characterized for all mineral phases. While some minerals, such as olivine and plagioclase, are known to readily react with CO<sub>2</sub> and form stable carbonate minerals, the reactivity of other minerals present in basalt, such as pyroxene and magnetite, is less understood [230,231]. Quantifying the reactivity of different minerals and their contribution to CO<sub>2</sub> mineralization is crucial for accurately predicting storage capacity. The kinetics of carbonation reactions in basalt formations are still not fully understood. The rates at which minerals react with CO<sub>2</sub> and convert into carbonates depend on factors such as temperature, pressure, water chemistry, and mineralogy [15,232,233].

#### *Future Directions for Research in Basalt Geochemistry for CO<sub>2</sub> Storage*

*Investigating the reactivity of underexplored minerals in basalt:* This research topic aims to explore the reactivity of minerals that are less understood in terms of their carbonation potential, such as pyroxene and magnetite. By conducting laboratory experiments and characterizing the reaction kinetics, researchers can determine the extent to which these minerals contribute to CO<sub>2</sub> mineralization in basalt formations.

*Quantifying the role of impurities in mineral reactivity:* This topic focuses on understanding the impact of impurities, such as clay minerals, sulfides, and organic matter, on the carbonation reactions in basalt. Researchers can study the interaction between these impurities and CO<sub>2</sub> to assess their catalytic or inhibitory effects on mineralization. This research will help refine the understanding of the overall reactivity of basalt minerals in the presence of impurities.

*Evaluating the influence of surface area of minerals on mineral reactivity:* Surface area of minerals play a vital role in mineral reactions. This research topic aims to investigate the effect of varying surface areas under varying fracture conditions and its effect on reactivity of basalt minerals towards CO<sub>2</sub>.

*Characterizing the carbonation pathways in basalt:* This topic involves studying the specific mechanisms and pathways through which CO<sub>2</sub> is incorporated into minerals during basalt mineralization. By employing advanced analytical techniques, researchers can track the transformation of minerals and identify the dominant carbonation pathways. This research will provide insights into the kinetics and reaction mechanisms involved in mineralization.

*Assessing the long-term stability of mineralized carbonates:* Understanding the long-term stability of CO<sub>2</sub> mineralization in basalt formations is crucial for assessing the permanence of storage. This research topic focuses on investigating the potential for mineral dissolution, reprecipitation, and alteration under various geological conditions over extended periods. By simulating long-term storage scenarios and conducting field observations, researchers can evaluate the durability and stability of the mineralized carbonates.

*Scaling up laboratory findings to field-scale applications:* This topic addresses the challenge of extrapolating laboratory results to field-scale CO<sub>2</sub> storage in basalt formations. It involves developing advanced modeling approaches to capture the scale-dependent effects, including fluid flow, heat transfer, and reactive transport processes. The research aims to improve the reliability of predictions and optimize the design and operation of large-scale basalt mineralization projects.

*Assessing the influence of temperature and pressure on mineral reactivity:* This research topic focuses on understanding how temperature and pressure conditions affect the reactivity of minerals in basalt formations. By conducting experiments at different temperature and pressure ranges representative of subsurface conditions, researchers can investigate the effect of these variables on the rate and extent of mineral carbonation. This knowledge will help refine predictions of CO<sub>2</sub> storage efficiency in basalt reservoirs.

*Investigating the influence of mineralogy on CO<sub>2</sub> trapping capacity:* This topic aims to explore how variations in basalt mineralogy, including mineral composition and crystalline structure, influence the capacity of the formation to trap and retain CO<sub>2</sub>. By comparing the reactivity and trapping efficiency of different mineral assemblages, researchers can identify mineralogical factors that enhance or hinder CO<sub>2</sub> storage. This research will contribute to optimizing site selection and reservoir characterization for basalt-based CO<sub>2</sub> storage.

These research topics address the gap in understanding the reactivity of basalt minerals for CO<sub>2</sub> mineralization and provide avenues for further investigation to improve the efficacy and predictability of basalt-based CO<sub>2</sub> storage technologies.

## 6. Conclusions

In conclusion, the study of basalt geochemistry and its influence on CO<sub>2</sub> trapping and retention is of paramount importance in understanding the mineralization potential of basalt formations. Through extensive research, the reactivity of different basalt minerals has been investigated, and a reactivity scale has been formulated to assess their carbonation potential. This understanding is crucial in determining the feasibility and efficiency of CO<sub>2</sub> storage in basalt reservoirs. By examining various factors such as mineral composition, grain size, surface area, and water chemistry, researchers have been able to elucidate the mechanisms and kinetics of mineralization reactions in basalt. The reactivity scale provides valuable insights into the relative carbonation rates of different minerals, allowing for the identification of highly reactive minerals that can maximize CO<sub>2</sub> uptake and storage. Moreover, the study of basalt geochemistry has revealed the complexities and uncertainties associated with geochemical processes and reactions involved in mineralization. Factors such as temperature, pressure, water–rock interactions, and impurities can significantly influence the efficiency and long-term stability of mineralized carbonates. Understanding these uncertainties is crucial for accurately predicting and optimizing CO<sub>2</sub> storage in basalt formations.

The research conducted on basalt reactivity and mineralization potential has paved the way for the development of effective strategies for carbon capture and storage. It provides a scientific basis for site selection, reservoir characterization, and the design of large-scale basalt mineralization projects. This knowledge is essential for mitigating climate change by safely and securely storing CO<sub>2</sub> in a stable mineral form.

In summary, the comprehensive study of basalt geochemistry and its impact on CO<sub>2</sub> trapping and retention has highlighted the importance of understanding mineral reactivity for assessing the mineralization potential of basalt formations. Through the formulation of a reactivity scale and investigation of geochemical processes, researchers have made significant strides in unraveling the complexities and uncertainties associated with basalt mineralization. This research lays the foundation for the development of efficient and sustainable carbon capture and storage technologies, contributing to global efforts to combat climate change.

**Author Contributions:** Conceptualization, M.H.R.; methodology, M.H.R.; writing—original draft preparation, M.H.R.; writing—review and editing, M.A.; supervision, M.A.; project administration, M.A.; funding acquisition, M.A. All authors have read and agreed to the published version of the manuscript.

**Funding:** The APC was funded by YUTP grant 015LC0-326.

**Data Availability Statement:** There is no data available.

**Acknowledgments:** The authors would like to acknowledge YUTP grant 015LC0-326 for providing financial support to carry out this review work.

**Conflicts of Interest:** The authors declare no conflict of interest.

## References

1. Kumar, S.; Srivastava, R.; Koh, J. Utilization of zeolites as CO<sub>2</sub> capturing agents: Advances and future perspectives. *J. CO<sub>2</sub> Util.* **2020**, *41*, 101251. [[CrossRef](#)]
2. Zhang, S.; Fan, Q.; Xia, R.; Meyer, T.J. CO<sub>2</sub> Reduction: From Homogeneous to Heterogeneous Electrocatalysis. *Accounts Chem. Res.* **2020**, *53*, 255–264. [[CrossRef](#)]
3. Huang, M.-T.; Zhai, P.-M. Achieving Paris Agreement temperature goals requires carbon neutrality by middle century with far-reaching transitions in the whole society. *Adv. Clim. Chang. Res.* **2021**, *12*, 281–286. [[CrossRef](#)]
4. Mikhaylov, A.; Moiseev, N.; Aleshin, K.; Burkhardt, T. Global climate change and greenhouse effect. *Entrep. Sustain. Issues* **2020**, *7*, 2897–2913. [[CrossRef](#)] [[PubMed](#)]
5. Schleussner, C.-F.; Ganti, G.; Rogelj, J.; Gidden, M.J. An emission pathway classification reflecting the Paris Agreement climate objectives. *Commun. Earth Environ.* **2022**, *3*, 135. [[CrossRef](#)]
6. Meinshausen, M.; Lewis, J.; McGlade, C.; Gütschow, J.; Nicholls, Z.; Burdon, R.; Cozzi, L.; Hackmann, B. Realization of Paris Agreement pledges may limit warming just below 2 °C. *Nature* **2022**, *604*, 304–309. [[CrossRef](#)]
7. Snæbjörnsdóttir, S.Ó.; Sigfússon, B.; Marieni, C.; Goldberg, D.; Gislason, S.R.; Oelkers, E.H. Carbon dioxide storage through mineral carbonation. *Nat. Rev. Earth Environ.* **2020**, *1*, 90–102. [[CrossRef](#)]
8. United Nations. *Paris Agreement*; Report of the Conference of the Parties to the United Nations Framework Convention on Climate Change; 55 International Legal Materials 743; HeinOnline: Getzville, NY, USA, 2017; Volume 4.
9. Zhang, Z.; Zheng, Y.; Qian, L.; Luo, D.; Dou, H.; Wen, G.; Yu, A.; Chen, Z. Emerging Trends in Sustainable CO<sub>2</sub>-Management Materials. *Adv. Mater.* **2022**, *34*, 2201547. [[CrossRef](#)]
10. Joachimski, M.M.; Müller, J.; Gallagher, T.M.; Mathes, G.; Chu, D.L.; Mouraviev, F.; Silantiev, V.; Sun, Y.D.; Tong, J.N. Five million years of high atmospheric CO<sub>2</sub> in the aftermath of the Permian-Triassic mass extinction. *Geology* **2022**, *50*, 650–654. [[CrossRef](#)]
11. Ali, M.; Yekeen, N.; Alanazi, A.; Keshavarz, A.; Iglauer, S.; Finkbeiner, T.; Hoteit, H. Saudi Arabian basalt/CO<sub>2</sub>/brine wettability: Implications for CO<sub>2</sub> geo-storage. *J. Energy Storage* **2023**, *62*, 106921. [[CrossRef](#)]
12. Kikuchi, S.; Wang, J.; Dandar, O.; Uno, M.; Watanabe, N.; Hirano, N.; Tsuchiya, N. NaHCO<sub>3</sub> as a carrier of CO<sub>2</sub> and its enhancement effect on mineralization during hydrothermal alteration of basalt. *Front. Environ. Sci.* **2023**, *11*, 199. [[CrossRef](#)]
13. Liu, D.; Agarwal, R.; Liu, F.; Yang, S.; Li, Y. Modeling and assessment of CO<sub>2</sub> geological storage in the Eastern Deccan Basalt of India. *Environ. Sci. Pollut. Res.* **2022**, *29*, 85465–85481. [[CrossRef](#)] [[PubMed](#)]
14. Raza, A.; Glatz, G.; Gholami, R.; Mahmoud, M.; Alafnan, S. Carbon mineralization and geological storage of CO<sub>2</sub> in basalt: Mechanisms and technical challenges. *Earth-Sci. Rev.* **2022**, *229*, 104036. [[CrossRef](#)]
15. Awolayo, A.N.; Laureijs, C.T.; Byng, J.; Luhmann, A.J.; Lauer, R.; Tutolo, B.M. Mineral surface area accessibility and sensitivity constraints on carbon mineralization in basaltic aquifers. *Geochim. Cosmochim. Acta* **2022**, *334*, 293–315. [[CrossRef](#)]
16. Radoman-Shaw, B.G.; Harvey, R.P.; Costa, G.; Jacobson, N.S.; Avishai, A.; Nakley, L.M.; Vento, D. Experiments on the reactivity of basaltic minerals and glasses in Venus surface conditions using the Glenn Extreme Environment Rig. *Meteorit. Planet. Sci.* **2022**, *57*, 1796–1819. [[CrossRef](#)]
17. Cao, R.; Muller, K.A.; Miller, Q.R.; White, M.D.; Bacon, D.H.; Schaef, H.T. Reactive Transport Modeling of Anthropogenic Carbon Mineralization in Stacked Columbia River Basalt Reservoirs. In Proceedings of the SPE/AAPG/SEG Unconventional Resources Technology Conference, Denver, CO, USA, 13–15 June 2023; p. D021S032R001.
18. Zhihao, G.; Changyou, X.; Songlin, L.; Xiaojie, Y.; Muxin, L.; Pengchun, L.; Xi, L.; Qing, D.; Xinwo, H. Progress of Methods for Assessing CO<sub>2</sub> Mineralization Storage Potential in Basalt. *Geol. J. China Univ.* **2023**, *29*, 66.
19. Snæbjörnsdóttir, S.; Gislason, S.R. CO<sub>2</sub> Storage Potential of Basaltic Rocks Offshore Iceland. *Energy Procedia* **2016**, *86*, 371–380. [[CrossRef](#)]
20. Goldberg, D.S.; Kent, D.V.; Olsen, P.E. Potential on-shore and off-shore reservoirs for CO<sub>2</sub> sequestration in Central Atlantic magmatic province basalts. *Proc. Natl. Acad. Sci. USA* **2010**, *107*, 1327–1332. [[CrossRef](#)]
21. Goldberg, D.; Slagle, A.L. A global assessment of deep-sea basalt sites for carbon sequestration. *Energy Procedia* **2009**, *1*, 3675–3682. [[CrossRef](#)]
22. Fisher, A.T. Permeability within basaltic oceanic crust. *Rev. Geophys.* **1998**, *36*, 143–182. [[CrossRef](#)]

23. Elderfield, H.; Wheat, C.; Mottl, M.; Monnin, C.; Spiro, B. Fluid and geochemical transport through oceanic crust: A transect across the eastern flank of the Juan de Fuca Ridge. *Earth Planet. Sci. Lett.* **1999**, *172*, 151–165. [[CrossRef](#)]
24. Seifritz, W. CO<sub>2</sub> disposal by means of silicates. *Nature* **1990**, *345*, 486. [[CrossRef](#)]
25. Matter, J.M.; Takahashi, T.; Goldberg, D. Experimental evaluation of in situ CO<sub>2</sub>-water-rock reactions during CO<sub>2</sub> injection in basaltic rocks: Implications for geological CO<sub>2</sub> sequestration. *Geochem. Geophys. Geosyst.* **2007**, *8*, 2. [[CrossRef](#)]
26. Wu, H.; Jayne, R.S.; Bodnar, R.J.; Pollyea, R.M. Simulation of CO<sub>2</sub> mineral trapping and permeability alteration in fractured basalt: Implications for geologic carbon sequestration in mafic reservoirs. *Int. J. Greenh. Gas Control* **2021**, *109*, 103383. [[CrossRef](#)]
27. Wang, G.; Mitchell, T.M.; Meredith, P.G.; Nara, Y.; Wu, Z. Influence of gouge thickness and grain size on permeability of macrofractured basalt. *J. Geophys. Res. Solid Earth* **2016**, *121*, 8472–8487. [[CrossRef](#)]
28. Nara, Y.; Meredith, P.G.; Yoneda, T.; Kaneko, K. Influence of macro-fractures and micro-fractures on permeability and elastic wave velocities in basalt at elevated pressure. *Tectonophysics* **2011**, *503*, 52–59. [[CrossRef](#)]
29. Christensen, N.I.; Ramanantoandro, R. Permeability of the oceanic crust based on experimental studies of basalt permeability at elevated pressures. *Tectonophysics* **1988**, *149*, 181–186. [[CrossRef](#)]
30. Vinciguerra, S.; Trovato, C.; Meredith, P.; Benson, P. Relating seismic velocities, thermal cracking and permeability in Mt. Etna and Iceland basalts. *Int. J. Rock Mech. Min. Sci.* **2005**, *42*, 900–910. [[CrossRef](#)]
31. Hosseini, M.; Ali, M.; Fahimpour, J.; Keshavarz, A.; Iglauer, S. Basalt-H<sub>2</sub>-brine wettability at geo-storage conditions: Implication for hydrogen storage in basaltic formations. *J. Energy Storage* **2022**, *52*, 104745. [[CrossRef](#)]
32. Al-Yaseri, A.; Ali, M.; Ali, M.; Taheri, R.; Wolff-Boenisch, D. Western Australia Basalt-CO<sub>2</sub>-Brine Wettability at Geo-Storage Conditions. *J. Colloid Interface Sci.* **2021**, *603*, 165–171. [[CrossRef](#)]
33. Wang, H.; Alvarado, V.; Bagdonas, D.A.; McLaughlin, J.F.; Kaszuba, J.P.; Grana, D.; Campbell, E.; Ng, K. Effect of CO<sub>2</sub>-brine-rock reactions on pore architecture and permeability in dolostone: Implications for CO<sub>2</sub> storage and EOR. *Int. J. Greenh. Gas Control* **2021**, *107*, 103283. [[CrossRef](#)]
34. Pearce, J.; Dawson, G.; Golab, A.; Knuefing, L.; Sommacal, S.; Rudolph, V.; Golding, S. A combined geochemical and  $\mu$ CT study on the CO<sub>2</sub> reactivity of Surat Basin reservoir and cap-rock cores: Porosity changes, mineral dissolution and fines migration. *Int. J. Greenh. Gas Control* **2018**, *80*, 10–24. [[CrossRef](#)]
35. Liu, D.; Agarwal, R.; Li, Y.; Yang, S. Reactive transport modeling of mineral carbonation in unaltered and altered basalts during CO<sub>2</sub> sequestration. *Int. J. Greenh. Gas Control* **2019**, *85*, 109–120. [[CrossRef](#)]
36. Gadikota, G. Multiphase carbon mineralization for the reactive separation of CO<sub>2</sub> and directed synthesis of H<sub>2</sub>. *Nat. Rev. Chem.* **2020**, *4*, 78–89. [[CrossRef](#)] [[PubMed](#)]
37. Gadikota, G.; Matter, J.; Kelemen, P.; Brady, P.V.; Park, A.-H.A. Elucidating the differences in the carbon mineralization behaviors of calcium and magnesium bearing aluminosilicates and magnesium silicates for CO<sub>2</sub> storage. *Fuel* **2020**, *277*, 117900. [[CrossRef](#)]
38. Loring, J.S.; Miller, Q.R.S.; Thompson, C.J.; Schaef, H.T. Chapter 4—Experimental Studies of Reactivity and Transformations of Rocks and Minerals in Water-Bearing Supercritical CO<sub>2</sub>. In *Science of Carbon Storage in Deep Saline Formations*; Newell, P., Ilgen, A.G., Eds.; Elsevier: Amsterdam, The Netherlands, 2019; pp. 63–88.
39. Bonto, M.; Welch, M.; Lüthje, M.; Andersen, S.; Veshareh, M.; Amour, F.; Afrough, A.; Mokhtari, R.; Hajiabadi, M.; Alizadeh, M.; et al. Challenges and enablers for large-scale CO<sub>2</sub> storage in chalk formations. *Earth Sci. Rev.* **2021**, *222*, 103826. [[CrossRef](#)]
40. Rasool, M.H.; Ahmad, M.; Ayoub, M. Selecting Geological Formations for CO<sub>2</sub> Storage: A Comparative Rating System. *Sustainability* **2023**, *15*, 6599. [[CrossRef](#)]
41. Menefee, A.H.; Li, P.; Giammar, D.E.; Ellis, B.R. Roles of Transport Limitations and Mineral Heterogeneity in Carbonation of Fractured Basalts. *Environ. Sci. Technol.* **2017**, *51*, 9352–9362. [[CrossRef](#)]
42. Liu, P.; Zhang, M.; Mo, L.; Zhong, J.; Xu, M.; Deng, M. Probe into carbonation mechanism of steel slag via FIB-TEM: The roles of various mineral phases. *Cem. Concr. Res.* **2022**, *162*, 106991. [[CrossRef](#)]
43. Kwak, J.H.; Hu, J.Z.; Turcu, R.V.; Rosso, K.M.; Ilton, E.S.; Wang, C.; Sears, J.A.; Engelhard, M.H.; Felmy, A.R.; Hoyt, D.W. The role of H<sub>2</sub>O in the carbonation of forsterite in supercritical CO<sub>2</sub>. *Int. J. Greenh. Gas Control* **2011**, *5*, 1081–1092. [[CrossRef](#)]
44. Wood, C.E.; Qafoku, O.; Loring, J.S.; Chaka, A.M. Role of Fe(II) Content in Olivine Carbonation in Wet Supercritical CO<sub>2</sub>. *Environ. Sci. Technol. Lett.* **2019**, *6*, 592–599. [[CrossRef](#)]
45. Yadav, S.; Mehra, A. A review on ex situ mineral carbonation. *Environ. Sci. Pollut. Res.* **2021**, *28*, 12202–12231. [[CrossRef](#)]
46. Wang, F.; Dreisinger, D.; Jarvis, M.; Hitchins, T. Kinetic evaluation of mineral carbonation of natural silicate samples. *Chem. Eng. J.* **2020**, *404*, 126522. [[CrossRef](#)]
47. Lu, X.; Carroll, K.J.; Turvey, C.C.; Dipple, G.M. Rate and capacity of cation release from ultramafic mine tailings for carbon capture and storage. *Appl. Geochem.* **2022**, *140*, 105285. [[CrossRef](#)]
48. Zheng, X.; Liu, J.; Wei, Y.; Li, K.; Yu, H.; Wang, X.; Ji, L.; Yan, S. Glycine-mediated leaching-mineralization cycle for CO<sub>2</sub> sequestration and CaCO<sub>3</sub> production from coal fly ash: Dual functions of glycine as a proton donor and receptor. *Chem. Eng. J.* **2022**, *440*, 135900. [[CrossRef](#)]
49. Wilcox, J. The Role of Mineral Carbonation in Carbon Capture. In *Carbon Capture*; Wilcox, J., Ed.; Springer New York: New York, NY, USA, 2012; pp. 257–273.
50. Ragipani, R.; Bhattacharya, S.; Suresh, A.K. A review on steel slag valorisation via mineral carbonation. *React. Chem. Eng.* **2021**, *6*, 1152–1178. [[CrossRef](#)]

51. Gadikota, G.; Matter, J.; Kelemen, P.; Park, A.-H.A. Chemical and morphological changes during olivine carbonation for CO<sub>2</sub> storage in the presence of NaCl and NaHCO<sub>3</sub>. *Phys. Chem. Chem. Phys.* **2013**, *16*, 4679–4693. [[CrossRef](#)]
52. Oelkers, E.H.; Gislason, S.R.; Matter, J. Mineral Carbonation of CO<sub>2</sub>. *Elements* **2008**, *4*, 333–337. [[CrossRef](#)]
53. Vienne, A.; Poblador, S.; Portillo-Estrada, M.; Hartmann, J.; Ijehon, S.; Wade, P.W.; Vicca, S. Enhanced weathering using basalt rock powder: Carbon sequestration, co-benefits and risks in a mesocosm study with *Solanum tuberosum*. *Front. Clim.* **2022**, *4*, 72. [[CrossRef](#)]
54. Goldberg, D.S.; Takahashi, T.; Slagle, A.L. Carbon dioxide sequestration in deep-sea basalt. *Proc. Natl. Acad. Sci. USA* **2008**, *105*, 9920–9925. [[CrossRef](#)]
55. Matter, J.M.; Broecker, W.S.; Gislason, S.R.; Gunnlaugsson, E.; Oelkers, E.H.; Stute, M.; Sigurdardóttir, H.; Stefánsson, A.; Alfreðsson, H.A.; Aradóttir, E.S.; et al. The CarbFix Pilot Project—storing carbon dioxide in basalt. *Energy Procedia* **2011**, *4*, 5579–5585. [[CrossRef](#)]
56. Hangx, S.J.; Spiers, C.J. Reaction of plagioclase feldspars with CO<sub>2</sub> under hydrothermal conditions. *Chem. Geol.* **2009**, *265*, 88–98. [[CrossRef](#)]
57. Nicholson, S. Carbon Removal to the Rescue? *Curr. Hist.* **2021**, *120*, 301–306. [[CrossRef](#)]
58. Gysi, A.P.; Stefánsson, A. Experiments and geochemical modeling of CO<sub>2</sub> sequestration during hydrothermal basalt alteration. *Chem. Geol.* **2012**, *306*, 10–28. [[CrossRef](#)]
59. Wu, Y.; Li, P. The potential of coupled carbon storage and geothermal extraction in a CO<sub>2</sub>-enhanced geothermal system: A review. *Geotherm. Energy* **2020**, *8*, 1–28. [[CrossRef](#)]
60. Huerta, N.J.; Cantrell, K.J.; White, S.K.; Brown, C.F. Hydraulic fracturing to enhance injectivity and storage capacity of CO<sub>2</sub> storage reservoirs: Benefits and risks. *Int. J. Greenh. Gas Control* **2020**, *100*, 103105. [[CrossRef](#)]
61. Wang, H.; Li, X.; Chen, Y.; Li, Z.; Hedding, D.W.; Nel, W.; Ji, J.; Chen, J. Geochemical behavior and potential health risk of heavy metals in basalt-derived agricultural soil and crops: A case study from Xuyi County, eastern China. *Sci. Total Environ.* **2020**, *729*, 139058. [[CrossRef](#)] [[PubMed](#)]
62. Hoyer, P.A.; Haase, K.M.; Regelous, M.; Fluteau, F. Systematic and Temporal Geochemical Changes in the Upper Deccan Lavas: Implications for the Magma Plumbing System of Flood Basalt Provinces. *Geochem. Geophys. Geosyst.* **2023**, *24*, e2022GC010750. [[CrossRef](#)]
63. Xia, L.; Li, X. Basalt geochemistry as a diagnostic indicator of tectonic setting. *Gondwana Res.* **2018**, *65*, 43–67. [[CrossRef](#)]
64. Stracke, A. A process-oriented approach to mantle geochemistry. *Chem. Geol.* **2021**, *579*, 120350. [[CrossRef](#)]
65. Zhang, Y.; Yu, K.; Fan, T.; Yue, Y.; Wang, R.; Jiang, W.; Xu, S.; Wang, Y. Geochemistry and petrogenesis of Quaternary basalts from Weizhou Island, northwestern South China Sea: Evidence for the Hainan plume. *Lithos* **2020**, *362*, 105493. [[CrossRef](#)]
66. Halder, M.; Paul, D.; Yang, S. Origin of silicic rocks of the Deccan Traps continental flood basalt province: Inferences from field observations, petrography, and geochemistry. *Geochemistry* **2023**, *83*, 125958. [[CrossRef](#)]
67. White, S.K.; Spane, F.A.; Schaef, H.T.; Miller, Q.R.S.; White, M.D.; Horner, J.A.; McGrail, B.P. Quantification of CO<sub>2</sub> Mineralization at the Wallula Basalt Pilot Project. *Environ. Sci. Technol.* **2020**, *54*, 14609–14616. [[CrossRef](#)] [[PubMed](#)]
68. Thorpe, M.T.; Hurowitz, J.A.; Dehouck, E. Sediment geochemistry and mineralogy from a glacial terrain river system in southwest Iceland. *Geochim. Cosmochim. Acta* **2019**, *263*, 140–166. [[CrossRef](#)]
69. Dai, Z.; Xu, L.; Xiao, T.; McPherson, B.; Zhang, X.; Zheng, L.; Dong, S.; Yang, Z.; Soltanian, M.R.; Yang, C.; et al. Reactive chemical transport simulations of geologic carbon sequestration: Methods and applications. *Earth-Sci. Rev.* **2020**, *208*, 103265. [[CrossRef](#)]
70. Soltanian, M.R.; Hajirezaie, S.; Hosseini, S.A.; Dashtian, H.; Amooie, M.A.; Meyal, A.; Ershadnia, R.; Ampomah, W.; Islam, A.; Zhang, X. Multicomponent reactive transport of carbon dioxide in fluvial heterogeneous aquifers. *J. Nat. Gas Sci. Eng.* **2019**, *65*, 212–223. [[CrossRef](#)]
71. Johnson, J.W.; Nitao, J.J.; Knauss, K.G. Reactive transport modelling of CO<sub>2</sub> storage in saline aquifers to elucidate fundamental processes, trapping mechanisms and sequestration partitioning. *Geol. Soc.* **2004**, *233*, 107–128. [[CrossRef](#)]
72. Rochelle, C.A.; Czernichowski-Lauriol, I.; Milodowski, A. The impact of chemical reactions on CO<sub>2</sub> storage in geological formations: A brief review. *Geol. Soc. Lond. Spec. Publ.* **2004**, *233*, 87–106. [[CrossRef](#)]
73. Xie, H.; Yue, H.; Zhu, J.; Liang, B.; Li, C.; Wang, Y.; Xie, L.; Zhou, X. Scientific and Engineering Progress in CO<sub>2</sub> Mineralization Using Industrial Waste and Natural Minerals. *Engineering* **2015**, *1*, 150–157. [[CrossRef](#)]
74. Jun, Y.-S.; Zhang, L.; Min, Y.; Li, Q. Nanoscale Chemical Processes Affecting Storage Capacities and Seals during Geologic CO<sub>2</sub> Sequestration. *Accounts Chem. Res.* **2017**, *50*, 1521–1529. [[CrossRef](#)]
75. Olajire, A.A. A review of mineral carbonation technology in sequestration of CO<sub>2</sub>. *J. Pet. Sci. Eng.* **2013**, *109*, 364–392. [[CrossRef](#)]
76. Chen, Z.-Y.; O'Connor, W.K.; Gerdemann, S. Chemistry of aqueous mineral carbonation for carbon sequestration and explanation of experimental results. *Environ. Prog.* **2006**, *25*, 161–166. [[CrossRef](#)]
77. Frey, F.A.; Green, D.H.; Roy, S.D. Integrated Models of Basalt Petrogenesis: A Study of Quartz Tholeiites to Olivine Melilitites from South Eastern Australia Utilizing Geochemical and Experimental Petrological Data. *J. Pet.* **1978**, *19*, 463–513. [[CrossRef](#)]
78. Chaussidon, M.; Jambon, A. Boron content and isotopic composition of oceanic basalts: Geochemical and cosmochemical implications. *Earth Planet. Sci. Lett.* **1994**, *121*, 277–291. [[CrossRef](#)]
79. Meen, J.K. Formation of shoshonites from calcalkaline basalt magmas: Geochemical and experimental constraints from the type locality. *Contrib. Miner. Pet.* **1987**, *97*, 333–351. [[CrossRef](#)]

80. Rhodes, J.M.; Vollinger, M.J. Composition of basaltic lavas sampled by phase-2 of the Hawaii Scientific Drilling Project: Geochemical stratigraphy and magma types. *Geochem. Geophys. Geosyst.* **2004**, *5*, 3. [[CrossRef](#)]
81. Doucet, L.S.; Tetley, M.G.; Li, Z.-X.; Liu, Y.; Gamaleldien, H. Geochemical fingerprinting of continental and oceanic basalts: A machine learning approach. *Earth-Sci. Rev.* **2022**, *233*, 104192. [[CrossRef](#)]
82. Ellam, R. Lithospheric thickness as a control on basalt geochemistry. *Geology* **1992**, *20*, 153–156. [[CrossRef](#)]
83. Hole, M.J.; LeMasurier, W.E. Tectonic controls on the geochemical composition of Cenozoic, mafic alkaline volcanic rocks from West Antarctica. *Contrib. Miner. Pet.* **1994**, *117*, 187–202. [[CrossRef](#)]
84. Richter, F.M.; Watson, E.B.; Mendybaev, R.; Dauphas, N.; Georg, B.; Watkins, J.; Valley, J. Isotopic fractionation of the major elements of molten basalt by chemical and thermal diffusion. *Geochim. Cosmochim. Acta* **2009**, *73*, 4250–4263. [[CrossRef](#)]
85. Yang, Z.; Li, J.; Jiang, Q.; Xu, F.; Guo, S.; Li, Y.; Zhang, J. Using Major Element Logratios to Recognize Compositional Patterns of Basalt: Implications for Source Lithological and Compositional Heterogeneities. *J. Geophys. Res. Solid Earth* **2019**, *124*, 3458–3490. [[CrossRef](#)]
86. Cone, K.A.; Palin, R.M.; Singha, K. Unsupervised machine learning with petrological database ApolloBasaltDB reveals complexity in lunar basalt major element oxide and mineral distribution patterns. *Icarus* **2020**, *346*, 113787. [[CrossRef](#)]
87. Ren, Q.; Li, M.; Han, S. Tectonic discrimination of olivine in basalt using data mining techniques based on major elements: A comparative study from multiple perspectives. *Big Earth Data* **2019**, *3*, 8–25. [[CrossRef](#)]
88. Niu, Y. Lithosphere thickness controls the extent of mantle melting, depth of melt extraction and basalt compositions in all tectonic settings on Earth—A review and new perspectives. *Earth-Sci. Rev.* **2021**, *217*, 103614. [[CrossRef](#)]
89. Yao, J.-H.; Zhu, W.-G.; Li, C.; Zhong, H.; Yu, S.; Ripley, E.M.; Bai, Z.-J. Olivine O isotope and trace element constraints on source variation of picrites in the Emeishan flood basalt province, SW China. *Lithos* **2019**, *338–339*, 87–98. [[CrossRef](#)]
90. Barnes, S.J.; Williams, M.; Smithies, R.H.; Hanski, E.; Lowrey, J.R. Trace Element Contents of Mantle-Derived Magmas Through Time. *J. Pet.* **2021**, *62*, egab024. [[CrossRef](#)]
91. Wang, J.; Zhou, H.; Salters, V.J.M.; Dick, H.J.B.; Standish, J.J.; Wang, C. Trace Element and Isotopic Evidence for Recycled Lithosphere from Basalts from 48 to 53 °E, Southwest Indian Ridge. *J. Pet.* **2020**, *61*, egaa068. [[CrossRef](#)]
92. Krein, S.B.; Behn, M.D.; Grove, T.L. Origins of Major Element, Trace Element, and Isotope Garnet Signatures in Mid-Ocean Ridge Basalts. *J. Geophys. Res. Solid Earth* **2020**, *125*, e2020JB019612. [[CrossRef](#)]
93. Wang, X.-J.; Chen, L.-H.; Hanyu, T.; Zhong, Y.; Shi, J.-H.; Liu, X.-W.; Kawabata, H.; Zeng, G.; Xie, L.-W. Magnesium isotopic fractionation during basalt differentiation as recorded by evolved magmas. *Earth Planet. Sci. Lett.* **2021**, *565*, 116954. [[CrossRef](#)]
94. Gong, Y.; Zeng, Z.; Cheng, W.; Lu, Y.; Zhang, L.; Yu, H.; Huang, F. Barium isotopic fractionation during strong weathering of basalt in a tropical climate. *Environ. Int.* **2020**, *143*, 105896. [[CrossRef](#)]
95. Bonnand, P.; Doucelance, R.; Boyet, M.; Bachèlery, P.; Bosq, C.; Auclair, D.; Schiano, P. The influence of igneous processes on the chromium isotopic compositions of Ocean Island basalts. *Earth Planet. Sci. Lett.* **2019**, *532*, 116028. [[CrossRef](#)]
96. Chen, S.; Sun, P.; Niu, Y.; Guo, P.; Elliott, T.; Hin, R.C. Molybdenum isotope systematics of lavas from the East Pacific Rise: Constraints on the source of enriched mid-ocean ridge basalt. *Earth Planet. Sci. Lett.* **2021**, *578*, 117283. [[CrossRef](#)]
97. Ma, L.; Xu, Y.-G.; Li, J.; Chen, L.-H.; Liu, J.-Q.; Li, H.-Y.; Huang, X.-L.; Ma, Q.; Hong, L.-B.; Wang, Y. Molybdenum isotopic constraints on the origin of EM1-type continental intraplate basalts. *Geochim. Cosmochim. Acta* **2021**, *317*, 255–268. [[CrossRef](#)]
98. Rasool, M.H.; Ahmad, M.; Ayoub, M.; Abbas, M.A. A Novel Ascorbic Acid Based Natural Deep Eutectic Solvent as a Drilling Mud Additive for Shale Stabilization. *Processes* **2023**, *11*, 1135. [[CrossRef](#)]
99. Rasool, M.H.; Zamir, A.; Elraies, K.A.; Ahmad, M.; Ayoub, M.; Abbas, M.A.; Ali, I. Rheological characterization of potassium carbonate deep eutectic solvent (DES) based drilling mud. *J. Pet. Explor. Prod. Technol.* **2021**, *12*, 1785–1795. [[CrossRef](#)]
100. Rasool, M.H.; Ahmad, M.; Ayoub, M.; Zamir, A.; Abbas, M.A. A review of the usage of deep eutectic solvents as shale inhibitors in drilling mud. *J. Mol. Liq.* **2022**, *361*, 119673. [[CrossRef](#)]
101. Rasool, M.H.; Zamir, A.; Elraies, K.A.; Ahmad, M.; Ayoub, M.; Abbas, M.A. Potassium carbonate based deep eutectic solvent (DES) as a potential drilling fluid additive in deep water drilling applications. *Pet. Sci. Technol.* **2021**, *39*, 612–631. [[CrossRef](#)]
102. Rasool, M.H.; Zamir, A.; Elraies, K.A.; Ahmad, M.; Ayoub, M.; Abbas, M.A. A Deep Eutectic Solvent based novel drilling mud with modified rheology for hydrates inhibition in deep water drilling. *J. Pet. Sci. Eng.* **2022**, *211*, 110151. [[CrossRef](#)]
103. A Descriptive Petrography of the Igneous Rocks. *Nature* **1938**, *142*, 495–496. [[CrossRef](#)]
104. Howie, R.A. R.W. Lemaitre (Ed.), A. Streckeisen, B. Zanettin, M.J. Le Bas, B. Bonin, P. Bateman, G. Bellieni, A. Dudel, S. Efreмова, A.J. Keller, J. Lameyre, P.A. Sabine, R. Schmid, H. Sørensen and A.R. Woolley *Igneous Rocks: A Classification and Glossary of Terms*. 2nd Edition. Cambridge (Cambridge University Press), 2002, xvi + 236 pp. Price £45.00. ISBN 0 521 66215 X. *Miner. Mag.* **2002**, *66*, 623–624. [[CrossRef](#)]
105. Rock, N.M. The nature and origin of lamprophyres: An overview. *Geol. Soc.* **1987**, *30*, 191–226. [[CrossRef](#)]
106. Middlemost, E.A.K. Naming materials in the magma/igneous rock system. *Earth Sci. Rev.* **1994**, *37*, 215–224. [[CrossRef](#)]
107. Streckeisen, A. Classification and nomenclature of volcanic rocks, lamprophyres, carbonatites and melilitic rocks IUGS Subcommittee on the Systematics of Igneous Rocks. *Int. J. Earth Sci.* **1980**, *69*, 194–207. [[CrossRef](#)]
108. Schmidt, S.T. (Ed.) *Igneous Rocks: Some Basic Concepts*. In *Transmitted Light Microscopy of Rock-Forming Minerals: An Introduction to Optical Mineralogy*; Springer International Publishing: Cham, Switzerland, 2023; pp. 145–160.
109. Verma, S.P.; Torres-Alvarado, I.S.; Sotelo-Rodríguez, Z.T. SINCLAS: Standard igneous norm and volcanic rock classification system. *Comput. Geosci.* **2002**, *28*, 711–715. [[CrossRef](#)]

110. Le Maitre, R.W. A proposal by the IUGS Subcommittee on the Systematics of Igneous Rocks for a chemical classification of volcanic rocks based on the total alkali silica (TAS) diagram. *Aust. J. Earth Sci.* **1984**, *31*, 243–255. [[CrossRef](#)]
111. Sun, S.S.; Hanson, G.N. Evolution of the mantle: Geochemical evidence from alkali basalt. *Geology* **1975**, *3*, 297–302. [[CrossRef](#)]
112. Fitton, J.; Dunlop, H. The Cameroon line, West Africa, and its bearing on the origin of oceanic and continental alkali basalt. *Earth Planet. Sci. Lett.* **1985**, *72*, 23–38. [[CrossRef](#)]
113. Hinton, R.; Upton, B. The chemistry of zircon: Variations within and between large crystals from syenite and alkali basalt xenoliths. *Geochim. Cosmochim. Acta* **1991**, *55*, 3287–3302. [[CrossRef](#)]
114. Wang, Z.-Z.; Liu, S.-A. Evolution of Intraplate Alkaline to Tholeiitic Basalts via Interaction Between Carbonated Melt and Lithospheric Mantle. *J. Pet.* **2021**, *62*, egab025. [[CrossRef](#)]
115. Manu Prasanth, M.; Hari, K.; Santosh, M. Tholeiitic basalts of Deccan large igneous province, India: An overview. *Geol. J.* **2019**, *54*, 2980–2993. [[CrossRef](#)]
116. Lang, S.; Mollo, S.; France, L.; Misiti, V.; Nazzari, M. Partitioning of Ti, Al, P, and Cr between olivine and a tholeiitic basaltic melt: Insights on olivine zoning patterns and cation substitution reactions under variable cooling rate conditions. *Chem. Geol.* **2022**, *601*, 120870. [[CrossRef](#)]
117. Lemdjou, Y.B.; Zhang, D.; Tchouankoue, J.P.; Hu, J.; Ngongang, N.B.T.; Tamehe, L.S.; Yuan, Y. Elemental and Sr–Nd–Pb isotopic compositions, and K–Ar ages of transitional and alkaline plateau basalts from the eastern edge of the West Cameroon Highlands (Cameroon Volcanic Line). *Lithos* **2020**, *358*, 105414. [[CrossRef](#)]
118. Kuepouo, G.; Tchouankoue, J.P.; Nagao, T.; Sato, H. Transitional tholeiitic basalts in the Tertiary Bana volcano–plutonic complex, Cameroon Line. *J. Afr. Earth Sci.* **2006**, *45*, 318–332. [[CrossRef](#)]
119. Zhao, C.; Qin, K.-Z.; Song, G.-X.; Li, G.-M.; Li, Z.-Z. Early Palaeozoic high-Mg basalt-andesite suite in the Duobaoshan Porphyry Cu deposit, NE China: Constraints on petrogenesis, mineralization, and tectonic setting. *Gondwana Res.* **2019**, *71*, 91–116. [[CrossRef](#)]
120. Fisk, M.R. Basalt magma interaction with harzburgite and the formation of high-magnesium andesites. *Geophys. Res. Lett.* **1986**, *13*, 467–470. [[CrossRef](#)]
121. Cervantes, P.; Wallace, P.J. Role of H<sub>2</sub>O in subduction-zone magmatism: New insights from melt inclusions in high-Mg basalts from central Mexico. *Geology* **2003**, *31*, 235–238. [[CrossRef](#)]
122. Scheffler, C.; Förster, T.; Mäder, E.; Heinrich, G.; Hempel, S.; Mechtcherine, V. Aging of alkali-resistant glass and basalt fibers in alkaline solutions: Evaluation of the failure stress by Weibull distribution function. *J. Non-Cryst. Solids* **2009**, *355*, 2588–2595. [[CrossRef](#)]
123. Sheth, H.C.; Torres-Alvarado, I.S.; Verma, S.P. What Is the “Calc-alkaline Rock Series”? *Int. Geol. Rev.* **2002**, *44*, 686–701. [[CrossRef](#)]
124. Pichavant, M.; Mysen, B.; Macdonald, R. Source and H<sub>2</sub>O content of high-MgO magmas in island arc settings: An experimental study of a primitive calc-alkaline basalt from St. Vincent, Lesser Antilles arc. *Geochim. Cosmochim. Acta* **2002**, *66*, 2193–2209. [[CrossRef](#)]
125. Weaver, B.L. The origin of ocean island basalt end-member compositions: Trace element and isotopic constraints. *Earth Planet. Sci. Lett.* **1991**, *104*, 381–397. [[CrossRef](#)]
126. Pilet, S.; Hernandez, J.; Sylvester, P.; Poujol, M. The metasomatic alternative for ocean island basalt chemical heterogeneity. *Earth Planet. Sci. Lett.* **2005**, *236*, 148–166. [[CrossRef](#)]
127. Gleeson, M.L.; Gibson, S.A.; Williams, H.M. Novel insights from Fe-isotopes into the lithological heterogeneity of Ocean Island Basalts and plume-influenced MORBs. *Earth Planet. Sci. Lett.* **2020**, *535*, 116114. [[CrossRef](#)]
128. Perfit, M.; Gust, D.; Bence, A.; Arculus, R.; Taylor, S. Chemical characteristics of island-arc basalts: Implications for mantle sources. *Chem. Geol.* **1980**, *30*, 227–256. [[CrossRef](#)]
129. Stolz, A.J.; Jochum, K.P.; Spettel, B.; Hofmann, A.W. Fluid- and melt-related enrichment in the subarc mantle: Evidence from Nb/Ta variations in island-arc basalts. *Geology* **1996**, *24*, 587–590. [[CrossRef](#)]
130. Xu, Y.; Wang, Q.; Tang, G.; Wang, J.; Li, H.; Zhou, J.; Li, Q.; Qi, Y.; Liu, P.; Ma, L.; et al. The origin of arc basalts: New advances and remaining questions. *Sci. China Earth Sci.* **2020**, *63*, 1969–1991. [[CrossRef](#)]
131. Benhelal, E.; Rashid, M.I.; Rayson, M.; Brent, G.; Oliver, T.; Stockenhuber, M.; Kennedy, E. Direct aqueous carbonation of heat activated serpentine: Discovery of undesirable side reactions reducing process efficiency. *Appl. Energy* **2019**, *242*, 1369–1382. [[CrossRef](#)]
132. Wang, F.; Dreisinger, D.; Jarvis, M.; Hitchins, T. Kinetics and mechanism of mineral carbonation of olivine for CO<sub>2</sub> sequestration. *Miner. Eng.* **2019**, *131*, 185–197. [[CrossRef](#)]
133. Chen, Y.; Zhang, Y. Clinopyroxene dissolution in basaltic melt. *Geochim. Cosmochim. Acta* **2009**, *73*, 5730–5747. [[CrossRef](#)]
134. Davis, F.A.; Cottrell, E. Experimental investigation of basalt and peridotite oxybarometers: Implications for spinel thermodynamic models and Fe<sup>3+</sup> compatibility during generation of upper mantle melts. *Am. Miner.* **2018**, *103*, 1056–1067. [[CrossRef](#)]
135. Yudovskaya, M.A.; Costin, G.; Shilovskikh, V.; Chaplygin, I.; McCreesh, M.; Kinnaird, J. Bushveld symplectic and sieve-textured chromite is a result of coupled dissolution-precipitation: A comparison with xenocrystic chromite reactions in arc basalt. *Contrib. Mineral. Petrol.* **2019**, *174*, 74. [[CrossRef](#)]
136. Aldanmaz, E.; van Hinsbergen, D.J.; Yıldız-Yükseköl, Ö.; Schmidt, M.W.; McPhee, P.J.; Meisel, T.; Güçtekin, A.; Mason, P.R. Effects of reactive dissolution of orthopyroxene in producing incompatible element depleted melts and refractory mantle residues during early fore-arc spreading: Constraints from ophiolites in eastern Mediterranean. *Lithos* **2020**, *360*, 105438. [[CrossRef](#)]

137. Kimura, J.-I.; Sano, S. Reactive Melt Flow as the Origin of Residual Mantle Lithologies and Basalt Chemistries in Mid-Ocean Ridges: Implications from the Red Hills Peridotite, New Zealand. *J. Pet.* **2012**, *53*, 1637–1671. [[CrossRef](#)]
138. Utzmann, A.; Hansteen, T.; Schmincke, H. Trace element mobility during sub-seafloor alteration of basaltic glass from Ocean Drilling Program site 953 (off Gran Canaria). *Int. J. Earth Sci.* **2002**, *91*, 661–679. [[CrossRef](#)]
139. Lissenberg, C.J.; MacLeod, C.J. A Reactive Porous Flow Control on Mid-ocean Ridge Magmatic Evolution. *J. Pet.* **2016**, *57*, 2195–2220. [[CrossRef](#)]
140. Klunk, M.A.; Shah, Z.; Caetano, N.R.; Conceição, R.V.; Wander, P.R.; Dasgupta, S.; Das, M. CO<sub>2</sub> sequestration by magnesite mineralisation through interaction of Mg-brine and CO<sub>2</sub>: Integrated laboratory experiments and computerised geochemical modelling. *Int. J. Environ. Stud.* **2019**, *77*, 492–509. [[CrossRef](#)]
141. Voigt, M.; Marieni, C.; Baldermann, A.; Galeczka, I.M.; Wolff-Boenisch, D.; Oelkers, E.H.; Gislason, S.R. An experimental study of basalt–seawater–CO<sub>2</sub> interaction at 130 °C. *Geochim. Cosmochim. Acta* **2021**, *308*, 21–41. [[CrossRef](#)]
142. Schaef, H.T.; McGrail, B.P. Dissolution of Columbia River Basalt under mildly acidic conditions as a function of temperature: Experimental results relevant to the geological sequestration of carbon dioxide. *Appl. Geochem.* **2009**, *24*, 980–987. [[CrossRef](#)]
143. Schaef, H.; McGrail, B.; Owen, A. Carbonate mineralization of volcanic province basalts. *Int. J. Greenh. Gas Control* **2010**, *4*, 249–261. [[CrossRef](#)]
144. Donaldson, C.H. The rates of dissolution of olivine, plagioclase, and quartz in a basalt melt. *Mineral. Mag.* **1985**, *49*, 683–693. [[CrossRef](#)]
145. de Obeso, J.C.; Awolayo, A.N.; Nightingale, M.J.; Tan, C.; Tutolo, B.M. Experimental study on plagioclase dissolution rates at conditions relevant to mineral carbonation of seafloor basalts. *Chem. Geol.* **2023**, *620*, 121348. [[CrossRef](#)]
146. Pokrovsky, O.S.; Schott, J. Kinetics and mechanism of forsterite dissolution at 25 C and pH from 1 to 12. *Geochim. Et Cosmochim. Acta* **2000**, *64*, 3313–3325. [[CrossRef](#)]
147. Monasterio-Guillot, L.; Rodriguez-Navarro, C.; Ruiz-Agudo, E. Kinetics and Mechanisms of Acid-pH Weathering of Pyroxenes. *Geochem. Geophys. Geosyst.* **2021**, *22*, e2021GC009711. [[CrossRef](#)]
148. Feniak, M.W. Grain sizes and shapes of various minerals in igneous rocks. *Am. Mineral. J. Earth Planet. Mater.* **1944**, *29*, 415–421.
149. Molahid, V.L.M.; Kusin, F.M.; Hasan, S.N.M.S.; Ramli, N.A.A.; Abdullah, A.M. CO<sub>2</sub> Sequestration through Mineral Carbonation: Effect of Different Parameters on Carbonation of Fe-Rich Mine Waste Materials. *Processes* **2022**, *10*, 432. [[CrossRef](#)]
150. Alexander, G.; Maroto-Valer, M.M.; Gafarova-Aksoy, P. Evaluation of reaction variables in the dissolution of serpentine for mineral carbonation. *Fuel* **2007**, *86*, 273–281. [[CrossRef](#)]
151. Zarandi, A.E.; Larachi, F.; Beaudoin, G.; Plante, B.; Sciortino, M. Nesquehonite as a carbon sink in ambient mineral carbonation of ultramafic mining wastes. *Chem. Eng. J.* **2017**, *314*, 160–168. [[CrossRef](#)]
152. Zarandi, A.E.; Larachi, F.; Beaudoin, G.; Plante, B.; Sciortino, M. Ambient mineral carbonation of different lithologies of mafic to ultramafic mining wastes/tailings—A comparative study. *Int. J. Greenh. Gas Control* **2017**, *63*, 392–400. [[CrossRef](#)]
153. Harrison, A.L.; Power, I.M.; Dipple, G.M. Accelerated Carbonation of Brucite in Mine Tailings for Carbon Sequestration. *Environ. Sci. Technol.* **2012**, *47*, 126–134. [[CrossRef](#)]
154. Kelemen, P.B.; Matter, J.; Streit, E.E.; Rudge, J.F.; Curry, W.B.; Blusztajn, J. Rates and mechanisms of mineral carbonation in peridotite: Natural processes and recipes for enhanced, in situ CO<sub>2</sub> capture and storage. *Annu. Rev. Earth Planet. Sci.* **2011**, *39*, 545–576. [[CrossRef](#)]
155. Matter, J.M.; Kelemen, P.B. Permanent storage of carbon dioxide in geological reservoirs by mineral carbonation. *Nat. Geosci.* **2009**, *2*, 837–841. [[CrossRef](#)]
156. O'Connor, W.; Dahlin, D.; Rush, G.; Gerdemann, S.; Penner, L.; Nilsen, D. *Aqueous Mineral Carbonation; Final Report—DOE/ARC-TR-04-002*, U.S. Department of Energy: Washington, DC, USA, 2005.
157. Park, A.-H.A.; Fan, L.-S. CO<sub>2</sub> mineral sequestration: Physically activated dissolution of serpentine and pH swing process. *Chem. Eng. Sci.* **2004**, *59*, 5241–5247. [[CrossRef](#)]
158. Chizmeshya, A.V.; McKelvy, M.J.; Squires, K.; Carpenter, R.W.; Béarat, H. *A Novel Approach to Mineral Carbonation: Enhancing Carbonation while Avoiding Mineral Pretreatment Process Cost*; Arizona State University: Tempe, AZ, USA, 2007.
159. Béarat, H.; McKelvy, M.J.; Chizmeshya, A.V.G.; Gormley, D.; Nunez, R.; Carpenter, R.W.; Squires, K.; Wolf, G.H. Carbon Sequestration via Aqueous Olivine Mineral Carbonation: Role of Passivating Layer Formation. *Environ. Sci. Technol.* **2006**, *40*, 4802–4808. [[CrossRef](#)] [[PubMed](#)]
160. Bruni, J.; Canepa, M.; Chiodini, G.; Cioni, R.; Cipolli, F.; Longinelli, A.; Marini, L.; Ottonello, G.; Zuccolini, M.V. Irreversible water–rock mass transfer accompanying the generation of the neutral, Mg–HCO<sub>3</sub> and high-pH, Ca–OH spring waters of the Genova province, Italy. *Appl. Geochem.* **2002**, *17*, 455–474. [[CrossRef](#)]
161. Eikeland, E.; Blichfeld, A.B.; Tyrsted, C.; Jensen, A.; Iversen, B.B. Optimized Carbonation of Magnesium Silicate Mineral for CO<sub>2</sub> Storage. *ACS Appl. Mater. Interfaces* **2015**, *7*, 5258–5264. [[CrossRef](#)]
162. Lewis, A.L.; Sarkar, B.; Wade, P.; Kemp, S.J.; Hodson, M.E.; Taylor, L.L.; Yeong, K.L.; Davies, K.; Nelson, P.N.; Bird, M.I.; et al. Effects of mineralogy, chemistry and physical properties of basalts on carbon capture potential and plant-nutrient element release via enhanced weathering. *Appl. Geochem.* **2021**, *132*, 105023. [[CrossRef](#)]
163. Romanov, V.; Soong, Y.; Carney, C.; Rush, G.E.; Nielsen, B.; O'Connor, W. Mineralization of Carbon Dioxide: A Literature Review. *ChemBioEng Rev.* **2015**, *2*, 231–256. [[CrossRef](#)]

164. Geerlings, H.; Zevenhoven, R. CO<sub>2</sub> Mineralization—Bridge Between Storage and Utilization of CO<sub>2</sub>. *Annu. Rev. Chem. Biomol. Eng.* **2013**, *4*, 103–117. [[CrossRef](#)]
165. Paukert, A.N.; Matter, J.M.; Kelemen, P.B.; Shock, E.L.; Havig, J.R. Reaction path modeling of enhanced in situ CO<sub>2</sub> mineralization for carbon sequestration in the peridotite of the Samail Ophiolite, Sultanate of Oman. *Chem. Geol.* **2012**, *330–331*, 86–100. [[CrossRef](#)]
166. Kwon, S.; Fan, M.; DaCosta, H.F.; Russell, A.G. Factors affecting the direct mineralization of CO<sub>2</sub> with olivine. *J. Environ. Sci.* **2011**, *23*, 1233–1239. [[CrossRef](#)]
167. Wang, F.; Dreisinger, D.; Jarvis, M.; Hitchens, T.; Dyson, D. Quantifying kinetics of mineralization of carbon dioxide by olivine under moderate conditions. *Chem. Eng. J.* **2018**, *360*, 452–463. [[CrossRef](#)]
168. Zhang, S.; DePaolo, D.J. Rates of CO<sub>2</sub> Mineralization in Geological Carbon Storage. *Accounts Chem. Res.* **2017**, *50*, 2075–2084. [[CrossRef](#)]
169. Miller, Q.R.; Schaef, H.T.; Kaszuba, J.P.; Gadikota, G.; McGrail, B.P.; Rosso, K.M. Quantitative review of olivine carbonation kinetics: Reactivity trends, mechanistic insights, and research frontiers. *Environ. Sci. Technol. Lett.* **2019**, *6*, 431–442. [[CrossRef](#)]
170. Peuble, S.; Godard, M.; Luquot, L.; Andreani, M.; Martinez, I.; Gouze, P. CO<sub>2</sub> geological storage in olivine rich basaltic aquifers: New insights from reactive-percolation experiments. *Appl. Geochem.* **2015**, *52*, 174–190. [[CrossRef](#)]
171. Chenrai, P.; Jitmahantakul, S.; Bissen, R.; Assawincharoenkij, T. A preliminary assessment of geological CO<sub>2</sub> storage in the Khorat Plateau, Thailand. *Front. Energy Res.* **2022**, *10*, 909898. [[CrossRef](#)]
172. Zhang, G.-L.; Chen, L.-H.; Jackson, M.G.; Hofmann, A.W. Evolution of carbonated melt to alkali basalt in the South China Sea. *Nat. Geosci.* **2017**, *10*, 229–235. [[CrossRef](#)]
173. Lesne, P.; Scaillet, B.; Pichavant, M.; Beny, J.-M. The carbon dioxide solubility in alkali basalts: An experimental study. *Contrib. Miner. Pet.* **2010**, *162*, 153–168. [[CrossRef](#)]
174. Wass, S.Y. Multiple origins of clinopyroxenes in alkali basaltic rocks. *Lithos* **1979**, *12*, 115–132. [[CrossRef](#)]
175. Gudbrandsson, S.; Wolff-Boenisch, D.; Gislason, S.R.; Oelkers, E.H. An experimental study of crystalline basalt dissolution from 2 ≤ pH ≤ 11 and temperatures from 5 to 75 °C. *Geochim. Cosmochim. Acta* **2011**, *75*, 5496–5509. [[CrossRef](#)]
176. Duda, A.; Schmincke, H.-U. Polybaric differentiation of alkali basaltic magmas: Evidence from green-core clinopyroxenes (Eifel, FRG). *Contrib. Miner. Pet.* **1985**, *91*, 340–353. [[CrossRef](#)]
177. Arculus, R.J. Geology and geochemistry of the alkali basalt—Andesite association of Grenada, Lesser Antilles island arc. *GSA Bull.* **1976**, *87*, 612–624. [[CrossRef](#)]
178. Kumar, A.; Shrivastava, J.; Pathak, V. Mineral carbonation reactions under water-saturated, hydrothermal-like conditions and numerical simulations of CO<sub>2</sub> sequestration in tholeiitic basalt of the Eastern Deccan Volcanic Province, India. *Appl. Geochem.* **2017**, *84*, 87–104. [[CrossRef](#)]
179. Shishkina, T.; Botcharnikov, R.; Holtz, F.; Almeev, R.; Portnyagin, M. Solubility of H<sub>2</sub>O- and CO<sub>2</sub>-bearing fluids in tholeiitic basalts at pressures up to 500MPa. *Chem. Geol.* **2010**, *277*, 115–125. [[CrossRef](#)]
180. Kumar, A.; Shrivastava, J.P. Carbon capture induced changes in Deccan basalt: A mass-balance approach. *Greenh. Gases Sci. Technol.* **2019**, *9*, 1158–1180. [[CrossRef](#)]
181. Aubaud, C.; Pineau, F.; Jambon, A.; Javoy, M. Kinetic disequilibrium of C, He, Ar and carbon isotopes during degassing of mid-ocean ridge basalts. *Earth Planet. Sci. Lett.* **2004**, *222*, 391–406. [[CrossRef](#)]
182. Dasgupta, R.; Chi, H.; Shimizu, N.; Buono, A.S.; Walker, D. Carbon solution and partitioning between metallic and silicate melts in a shallow magma ocean: Implications for the origin and distribution of terrestrial carbon. *Geochim. Cosmochim. Acta* **2012**, *102*, 191–212. [[CrossRef](#)]
183. Rigopoulos, I.; Petalidou, K.C.; Vasiliades, M.A.; Delimitis, A.; Ioannou, I.; Efstathiou, A.M.; Kyratsi, T. Carbon dioxide storage in olivine basalts: Effect of ball milling process. *Powder Technol.* **2015**, *273*, 220–229. [[CrossRef](#)]
184. Clague, D.A.; Dixon, J.E. Extrinsic controls on the evolution of Hawaiian ocean island volcanoes. *Geochem. Geophys. Geosyst.* **2000**, *1*, 4. [[CrossRef](#)]
185. Hodson, A.; Tranter, M.; Vatne, G. Contemporary rates of chemical denudation and atmospheric CO<sub>2</sub> sequestration in glacier basins: An Arctic perspective. *Earth Surf. Process. Landforms* **2000**, *25*, 1447–1471. [[CrossRef](#)]
186. Kanakiya, S.; Adam, L.; Esteban, L.; Rowe, M.C.; Shane, P. Dissolution and secondary mineral precipitation in basalts due to reactions with carbonic acid. *J. Geophys. Res. Solid Earth* **2017**, *122*, 4312–4327. [[CrossRef](#)]
187. Hsieh, P.-S.; Tien, N.-C.; Lin, C.-K.; Lin, W.; Lu, H.-Y. A multi-sequestration concept of CO<sub>2</sub> geological storage: Shale-Sandstone-Basalt system in Northwestern Taiwan. *Int. J. Greenh. Gas Control* **2017**, *64*, 137–151. [[CrossRef](#)]
188. Gysi, A.P.; Stefánsson, A. Mineralogical aspects of CO<sub>2</sub> sequestration during hydrothermal basalt alteration—An experimental study at 75 to 250 °C and elevated pCO<sub>2</sub>. *Chem. Geol.* **2012**, *306–307*, 146–159. [[CrossRef](#)]
189. Gysi, A.P.; Stefánsson, A. CO<sub>2</sub>-water-basalt interaction. Low temperature experiments and implications for CO<sub>2</sub> sequestration into basalts. *Geochim. Cosmochim. Acta* **2011**, *81*, 129–152. [[CrossRef](#)]
190. Rosenbauer, R.J.; Thomas, B.; Bischoff, J.L.; Palandri, J. Carbon sequestration via reaction with basaltic rocks: Geochemical modeling and experimental results. *Geochim. Cosmochim. Acta* **2012**, *89*, 116–133. [[CrossRef](#)]
191. McGrail, B.; Spane, F.; Amonette, J.; Thompson, C.; Brown, C. Injection and Monitoring at the Wallula Basalt Pilot Project. *Energy Procedia* **2014**, *63*, 2939–2948. [[CrossRef](#)]

192. Kelland, M.E.; Wade, P.W.; Lewis, A.L.; Taylor, L.L.; Sarkar, B.; Andrews, M.G.; Lomas, M.R.; Cotton, T.E.A.; Kemp, S.J.; James, R.H.; et al. Increased yield and CO<sub>2</sub> sequestration potential with the C<sub>4</sub> cereal *Sorghum bicolor* cultivated in basaltic rock dust-amended agricultural soil. *Glob. Chang. Biol.* **2020**, *26*, 3658–3676. [[CrossRef](#)]
193. von Strandmann, P.A.P.; Burton, K.W.; James, R.H.; van Calsteren, P.; Gislason, S.R.; Sigfússon, B. The influence of weathering processes on riverine magnesium isotopes in a basaltic terrain. *Earth Planet. Sci. Lett.* **2008**, *276*, 187–197. [[CrossRef](#)]
194. Karkalis, C.; Magganas, A.; Koutsovitis, P.; Pomonis, P.; Ntaflos, T. Multiple Rodingitization Stages in Alkaline, Tholeiitic, and Calc-Alkaline Basaltic Dikes Intruding Exhumed Serpentinized Tethyan Mantle from Evia Island, Greece. *Lithosphere* **2022**, *2022*, 9507697. [[CrossRef](#)]
195. Deng, H.; Kusky, T.; Bozurt, E.; Chen, C.; Wang, L.; Dong, Z.; Meng, J. Sr-Nd-Ca isotopic variations of Cenozoic calc-alkaline and alkaline volcanic rocks above a slab tear in Western Anatolia, Turkey. *GSA Bull.* **2023**. [[CrossRef](#)]
196. Currie, K.; Williams, P. An Archean calc-alkaline lamprophyre suite, northeastern Yilgarn Block, western Australia. *Lithos* **1993**, *31*, 33–50. [[CrossRef](#)]
197. Yang, W.-B.; Niu, H.-C.; Shan, Q.; Luo, Y.; Sun, W.-D.; Li, C.-Y.; Li, N.-B.; Yu, X.-Y. Late Paleozoic calc-alkaline to shoshonitic magmatism and its geodynamic implications, Yuximolegai area, western Tianshan, Xinjiang. *Gondwana Res.* **2012**, *22*, 325–340. [[CrossRef](#)]
198. Akinin, V.V.; Miller, E.L. Evolution of calc-alkaline magmas of the Okhotsk-Chukotka volcanic belt. *Petrology* **2011**, *19*, 237–277. [[CrossRef](#)]
199. Choi, E.; Fiorentini, M.L.; Giuliani, A.; Foley, S.F.; Maas, R.; Taylor, W.R. Subduction-related petrogenesis of Late Archean calc-alkaline lamprophyres in the Yilgarn Craton (Western Australia). *Precambrian Res.* **2019**, *338*, 105550. [[CrossRef](#)]
200. Kirstein, L.A.; Walowski, K.J.; Jones, R.E.; Burgess, R.; Fitton, J.G.; De Hoog, J.C.M.; Savov, I.P.; Kalnins, L.M.; EIMF. Volatiles and Intraplate Magmatism: A Variable Role for Carbonated and Altered Oceanic Lithosphere in Ocean Island Basalt Formation. *J. Pet.* **2023**, *64*, egad022. [[CrossRef](#)]
201. Dasgupta, R.; Hirschmann, M.M.; Smith, N.D. Partial Melting Experiments of Peridotite + CO<sub>2</sub> at 3 GPa and Genesis of Alkalic Ocean Island Basalts. *J. Petrol.* **2007**, *48*, 2093–2124. [[CrossRef](#)]
202. Rosenthal, A.; Hauri, E.; Hirschmann, M. Experimental determination of C, F, and H partitioning between mantle minerals and carbonated basalt, CO<sub>2</sub>/Ba and CO<sub>2</sub>/Nb systematics of partial melting, and the CO<sub>2</sub> contents of basaltic source regions. *Earth Planet. Sci. Lett.* **2015**, *412*, 77–87. [[CrossRef](#)]
203. Mallik, A.; Dasgupta, R. Effect of variable CO<sub>2</sub> on eclogite-derived andesite and lherzolite reaction at 3 GPa—Implications for mantle source characteristics of alkalic ocean island basalts. *Geochem. Geophys. Geosyst.* **2014**, *15*, 1533–1557. [[CrossRef](#)]
204. Hanyu, T.; Shimizu, K.; Ushikubo, T.; Kimura, J.-I.; Chang, Q.; Hamada, M.; Ito, M.; Iwamori, H.; Ishikawa, T. Tiny droplets of ocean island basalts unveil Earth’s deep chlorine cycle. *Nat. Commun.* **2019**, *10*, 60. [[CrossRef](#)]
205. Liu, S.-A.; Wang, Z.-Z.; Li, S.-G.; Huang, J.; Yang, W. Zinc isotope evidence for a large-scale carbonated mantle beneath eastern China. *Earth Planet. Sci. Lett.* **2016**, *444*, 169–178. [[CrossRef](#)]
206. Parkinson, I.J.; Arculus, R.J.; Eggins, S.M. Peridotite xenoliths from Grenada, Lesser Antilles Island Arc. *Contrib. Miner. Pet.* **2003**, *146*, 241–262. [[CrossRef](#)]
207. Foley, S.F.; Wheller, G.E. Parallels in the origin of the geochemical signatures of island arc volcanics and continental potassic igneous rocks: The role of residual titanates. *Chem. Geol.* **1990**, *85*, 1–18. [[CrossRef](#)]
208. Ben Othman, D.; White, W.M.; Patchett, J. The geochemistry of marine sediments, island arc magma genesis, and crust-mantle recycling. *Earth Planet. Sci. Lett.* **1989**, *94*, 1–21. [[CrossRef](#)]
209. Wang, S.-J.; Li, S.-G. Magnesium isotope geochemistry of the carbonate-silicate system in subduction zones. *Natl. Sci. Rev.* **2022**, *9*, nwac036. [[CrossRef](#)] [[PubMed](#)]
210. Menefee, A.H.; Giammar, D.E.; Ellis, B.R. Permanent CO<sub>2</sub> Trapping through Localized and Chemical Gradient-Driven Basalt Carbonation. *Environ. Sci. Technol.* **2018**, *52*, 8954–8964. [[CrossRef](#)] [[PubMed](#)]
211. Das, A.; Krishnaswami, S. Elemental geochemistry of river sediments from the Deccan Traps, India: Implications to sources of elements and their mobility during basalt–water interaction. *Chem. Geol.* **2007**, *242*, 232–254. [[CrossRef](#)]
212. Garcia, B.; Beaumont, V.; Perfetti, E.; Rouchon, V.; Blanchet, D.; Oger, P.; Dromart, G.; Huc, A.-Y.; Haeseler, F. Experiments and geochemical modelling of CO<sub>2</sub> sequestration by olivine: Potential, quantification. *Appl. Geochem.* **2010**, *25*, 1383–1396. [[CrossRef](#)]
213. Gupta, H.; Chakrapani, G.J.; Selvaraj, K.; Kao, S.-J. The fluvial geochemistry, contributions of silicate, carbonate and saline–alkaline components to chemical weathering flux and controlling parameters: Narmada River (Deccan Traps), India. *Geochim. Cosmochim. Acta* **2011**, *75*, 800–824. [[CrossRef](#)]
214. Harvey, O.R.; Qafoku, N.P.; Cantrell, K.J.; Lee, G.; Amonette, J.E.; Brown, C.F. Geochemical Implications of Gas Leakage associated with Geologic CO<sub>2</sub> Storage—A Qualitative Review. *Environ. Sci. Technol.* **2012**, *47*, 23–36. [[CrossRef](#)]
215. Van Pham, T.H.; Aagaard, P.; Hellevang, H. On the potential for CO<sub>2</sub> mineral storage in continental flood basalts—PHREEQC batch- and 1D diffusion–reaction simulations. *Geochem. Trans.* **2012**, *13*, 5. [[CrossRef](#)]
216. Koukouzas, N.; Koutsovitis, P.; Tyrologou, P.; Karkalis, C.; Arvanitis, A. Potential for Mineral Carbonation of CO<sub>2</sub> in Pleistocene Basaltic Rocks in Volos Region (Central Greece). *Minerals* **2019**, *9*, 627. [[CrossRef](#)]
217. Rowe, M.C.; Carey, R.J.; White, J.D.L.; Kilgour, G.; Hughes, E.; Ellis, B.; Rosseel, J.-B.; Segovia, A. Tarawera 1886: An integrated review of volcanological and geochemical characteristics of a complex basaltic eruption. *N. Z. J. Geol. Geophys.* **2021**, *64*, 296–319. [[CrossRef](#)]

218. Nicholson, K.; Black, P.; Picard, C. Geochemistry and tectonic significance of the Tangihua Ophiolite Complex, New Zealand. *Tectonophysics* **2000**, *321*, 1–15. [[CrossRef](#)]
219. Castillo, P.R.; Janney, P.E.; Solidum, R.U. Petrology and geochemistry of Camiguin Island, southern Philippines: Insights to the source of adakites and other lavas in a complex arc setting. *Contrib. Miner. Pet.* **1999**, *134*, 33–51. [[CrossRef](#)]
220. Safonova, I.Y.; Utsunomiya, A.; Kojima, S.; Nakae, S.; Tomurtogoo, O.; Filippov, A.; Koizumi, K. Pacific superplume-related oceanic basalts hosted by accretionary complexes of Central Asia, Russian Far East and Japan. *Gondwana Res.* **2009**, *16*, 587–608. [[CrossRef](#)]
221. Ragnheidardottir, E.; Sigurdardottir, H.; Kristjansdottir, H.; Harvey, W. Opportunities and challenges for CarbFix: An evaluation of capacities and costs for the pilot scale mineralization sequestration project at Hellisheidi, Iceland and beyond. *Int. J. Greenh. Gas Control* **2011**, *5*, 1065–1072. [[CrossRef](#)]
222. Kelemen, P.; Benson, S.M.; Pilorgé, H.; Psarras, P.; Wilcox, J. An Overview of the Status and Challenges of CO<sub>2</sub> Storage in Minerals and Geological Formations. *Front. Clim.* **2019**, *1*, 9. [[CrossRef](#)]
223. Gysi, A.P. Numerical simulations of CO<sub>2</sub> sequestration in basaltic rock formations: Challenges for optimizing mineral-fluid reactions. *Pure Appl. Chem.* **2017**, *89*, 581–596. [[CrossRef](#)]
224. Singh, R.K.; Nayak, N.P. Complications in drilling operations in basalt for CO<sub>2</sub> sequestration: An overview. *Mater. Today Proc.* **2023**, *in press*. [[CrossRef](#)]
225. McGrail, B.P.; Schaef, H.T.; Ho, A.M.; Chien, Y.-J.; Dooley, J.J.; Davidson, C.L. Potential for carbon dioxide sequestration in flood basalts. *J. Geophys. Res. Solid Earth* **2006**, *111*, B12. [[CrossRef](#)]
226. Sigfusson, B.; Gislason, S.R.; Matter, J.M.; Stute, M.; Gunnlaugsson, E.; Gunnarsson, I.; Aradottir, E.S.; Sigurdardottir, H.; Mesfin, K.; Alfredsson, H.A.; et al. Solving the carbon-dioxide buoyancy challenge: The design and field testing of a dissolved CO<sub>2</sub> injection system. *Int. J. Greenh. Gas Control* **2015**, *37*, 213–219. [[CrossRef](#)]
227. Vishal, V.; Chandra, D.; Singh, U.; Verma, Y. Understanding initial opportunities and key challenges for CCUS deployment in India at scale. *Resour. Conserv. Recycl.* **2021**, *175*, 105829. [[CrossRef](#)]
228. Okoko, G.O.; Olaka, L.A. Can East African rift basalts sequester CO<sub>2</sub>? Case study of the Kenya rift. *Sci. Afr.* **2021**, *13*, e00924. [[CrossRef](#)]
229. Gupta, A.; Paul, A. Carbon capture and sequestration potential in India: A comprehensive review. *Energy Procedia* **2019**, *160*, 848–855. [[CrossRef](#)]
230. Khatiwada, M.; Adam, L.; Morrison, M.; van Wijk, K. A feasibility study of time-lapse seismic monitoring of CO<sub>2</sub> sequestration in a layered basalt reservoir. *J. Appl. Geophys.* **2012**, *82*, 145–152. [[CrossRef](#)]
231. Stauffer, P.H.; Keating, G.N.; Middleton, R.S.; Viswanathan, H.S.; Berchtold, K.A.; Singh, R.P.; Pawar, R.J.; Mancino, A. Greening Coal: Breakthroughs and Challenges in Carbon Capture and Storage. *Environ. Sci. Technol.* **2011**, *45*, 8597–8604. [[CrossRef](#)] [[PubMed](#)]
232. Adam, L.; van Wijk, K.; Otheim, T.; Batzle, M. Changes in elastic wave velocity and rock microstructure due to basalt-CO<sub>2</sub>-water reactions. *J. Geophys. Res. Solid Earth* **2013**, *118*, 4039–4047. [[CrossRef](#)]
233. Gysi, A.P.; Stefánsson, A. CO<sub>2</sub>-water-basalt interaction. Numerical simulation of low temperature CO<sub>2</sub> sequestration into basalts. *Geochim. Cosmochim. Acta* **2011**, *75*, 4728–4751. [[CrossRef](#)]

**Disclaimer/Publisher's Note:** The statements, opinions and data contained in all publications are solely those of the individual author(s) and contributor(s) and not of MDPI and/or the editor(s). MDPI and/or the editor(s) disclaim responsibility for any injury to people or property resulting from any ideas, methods, instructions or products referred to in the content.